Ocean Sci. Discuss., https://doi.org/10.5194/os-2017-74
Manuscript under review for journal Ocean Sci.
Discussion started: 4 October 2017

Ocean Science
Discussions
Open Access
EGU

Impact of intraseasonal wind bursts on SST variability in the far eastern Tropical Atlantic Ocean during boreal spring 2005 and 2006. Focus on the mid-May 2005 event.

Gaëlle Herbert[1], Bernard Bourlès[1]

[1]:Institut de Recherche pour le Développement (IRD), Laboratoire d'Etudes Géophysiques et Océanographie Spatiale (LEGOS), Brest, France.

Correspondence to: Gaëlle Herbert (gaelle.herbert@ird.fr)

Abstract. The impact of spring intraseasonal wind bursts on sea surface temperature variability in the eastern Tropical Atlantic Ocean in 2005 and 2006 is investigated using numerical simulation and observations. We specially focus on the few documented coastal region east of 5° E and between the equator and 7° S. For both years, the southerly winds strengthening induced cooling events through i) upwelling processes; ii) vertical mixing due to vertical shear of zonal current; and for some particular events iii) a decrease of incoming surface shortwave radiation. The strength of the cooling events was modulated by subsurface conditions affected by the arrival of Kelvin waves from the west influencing the depth of the thermocline. Once impinging the eastern boundary, the Kelvin waves excited westward-propagating Rossby waves which, combined with the effect of enhanced westward surface currents, contributed to the westward extension of the cold water. A particularly strong wind event occurred in mid-May 2005 and caused an anomalous strong cooling off Cape-Lopez and in the whole eastern Tropical Atlantic Ocean. From the analysis of oceanic and atmospheric conditions during this particular event, it appears that anomalous strong spring wind strengthening associated to anomalous strong Hadley cell activity made the event as a decisive event which prematurely triggered the rainfall coastal onset in the northern Gulf of Guinea. Results show that no similar atmospheric conditions were observed over the 1998-2008 period. It is also found that the anomalous oceanic and atmospheric conditions associated to the event exerted strong influence on rainfall off Northeast Brazil. This study highlights the different processes through which the wind power from South Atlantic is brought to the ocean in the Gulf of Guinea and emphasizes the need to further document and monitor the South Atlantic region.

1.Introduction

The eastern equatorial Atlantic Ocean shows a pronounced seasonal cycle in sea surface temperature (SST) (Wauthy, 1983; Mitchell and Wallace, 1992). One strong signature on the SST seasonal cycle in the eastern equatorial Atlantic is the Atlantic cold tongue (ACT) (Zebiak, 1993) characterized by a fast drop of SST (up to 7° C) in boreal spring and summer slightly south of the equator and east of 20°W (Merle, 1980; Picaut, 1983). During boreal summer, the southern boundary of this cooler temperature connects progressively with the austral

Ocean Sci. Discuss., https://doi.org/10.5194/os-2017-74
Manuscript under review for journal Ocean Sci.
Discussion started: 4 October 2017

winter cooling of the Southern hemisphere SSTs. A number of observational (Merle, 1980; Foltz et al., 2003) and modeling (Philander and Pacanowski, 1986; Yu et al., 2006; Peter et al., 2006) studies show that the development of the ACT is driven by the seasonal increase of the Southern Hemisphere trade winds during late boreal winter to early summer (Brandt et al., 2011) associated to the meridional displacement of the Inter-Tropical Convergence Zone (ITCZ) (Picaut, 1983; Colin, 1989; Waliser and Gautier, 1993; Nobre and Shukla, 1996). The equatorial cooling would be regulated by a coupling between thermocline shoaling, subsurface dynamics (Yu et al., 2006; Peter et al., 2006; Wade et al., 2011; Jouanno et al., 2011) including turbulent mixing, vertical advection and entrainment, as well as horizontal advection. The equatorial thermocline shoaling is the consequence of local and remote wind forcing: the strengthening of easterly winds in the western equatorial Atlantic remotely forces the seasonal upwelling in the eastern part of the basin via equatorial Kelvin waves (Moore et al., 1978; Adamec and O'Brien, 1978; Busalacchi and Picaut, 1983; McCreary et al., 1984).

Besides the dominant seasonal cycle, the eastern tropical Atlantic is under the influence of meridional southerly winds (Picaut, 1984) which fluctuate with a period close to 15 days (Krishnamurti, 1980; de Coëtlogon et al., 2010; Jouanno et al., 2013). These intraseasonal wind fluctuations are therefore expected to be a major contributor to the seasonal SST cooling and their fluctuations occur as a vector of energy and momentum from the South Atlantic to the eastern equatorial Atlantic. A connection between the strength of the St. Helena Anticyclone and SST anomalies in the southeastern tropical Atlantic has been described by Lübbecke et al. (2014). These authors suggest that the St. Helena Anticyclone variability might be an importance source of anomalous tropical Atlantic wind power which affects SST in the eastern equatorial Atlantic via several mechanisms: zonal wind stress changes in the western equatorial basin, wave adjustment, meridional advection of subsurface temperature anomalies, intraseasonal wind stress variations, and possibly even other mechanisms. Through the in situ data analysis of AMMA/EGEE cruises (Redelsperger et al., 2006; Bourlès et al., 2007) carried out in 2005 and 2006, Marin et al. (2009) show that the SST seasonal cooling at the equator east of 10° W is not smooth but results from the succession of short-duration cooling events generated by southeasterly wind bursts due to the fluctuating St. Helena Anticyclone. In addition, according to Leduc-Leballeur et al. (2013), the sharp and durable change in the atmospheric circulation in the northern Gulf of Guinea (durably strong southerlies north of equator) takes place through an abrupt seasonal transition prepared by a succession of southerly wind bursts and possibly triggered by a significantly stronger wind burst. The southerly wind bursts occurring in spring in the Gulf of Guinea thus would play an important role in driving precipitation pattern in the area through air-sea interactions (de Coëtlogon et al., 2010; Nicholson and Dezfuli, 2013) and coupling between the ACT and the West Africa Monsoon (WAM).

Improving our understanding of the impact of such wind bursts on SST variability at intraseasonal scale in the eastern Tropical Atlantic is important through its link with the regional climate. However, while the ACT and Angola-Benguela regions have been the object of many studies, the dynamics and SST variability of the coastal eastern region is much less documented.

Ocean Sci. Discuss., https://doi.org/10.5194/os-2017-74
Manuscript under review for journal Ocean Sci.
Discussion started: 4 October 2017

In this study, we therefore first focus our analysis off Cape-Lopez (defined from 0° N-7° S; 5° E-14° E and hereafter called CLR for 'Cape-Lopez region') and aim to improve understanding of its seasonal SST variability and the impact of intraseasonal winds on SST variability during spring and summer. To this end, we use regional high resolution model results as well as satellite SST data and sea surface height observations. We first use model outputs from 1998 to 2008 to analyze the seasonal cycle in CLR and to highlight its interannual variability, and then we specially focus on the years 2005 and 2006 to investigate the SST response of intraseasonal wind forcing. These two particular years were largely investigated during the African Monsoon Multidisciplinary Analyses (AMMA) experiment (Redelsperger et al., 2006). The year 2005 is characterized by the lowest SST values in the ACT during the past 3 decades (along with 1982), while 2006 is considered as a normal year (Caniaux et al., 2011). Also, 2005 exhibits the earliest development of the ACT. The study of SST variability at intraseasonal scale during these two years is thus interesting for better understanding their observed differences in SST seasonal conditions. These two particular years have been also chosen by Marin et al. (2009) to study the variability of the properties of the ACT. Their study concerned the equatorial area west of 4° E, whereas we propose to focus in CLR, east of 5° E where coastal processes are expected to be involved.

Most studies on CLR focused on the analysis of observational dataset to examine the hydrology and its seasonal variation along the frontal (coastal) region of Congo (e.g. Merle, 1972; Piton, 1988) or on the impact of Congo River on SST and mixed layer (e.g. Materia et al., 2012; Denamiel et al., 2013; White and Toumi, 2014) but, to our knowledge, no detailed analysis of SST variability at seasonal and intraseasonal time scales have been realized. A better understanding of ocean-atmosphere interactions in this region is thus needed. Some previous studies related to the whole eastern Tropical Atlantic (Gulf of Guinea) suggest that multiplicity of processes could be in play in CLR, coupling remote and local forcing, and combined with the very low thermal inertia of the mixed layer depth. For example, Giordani et al. (2013) show from regional model results that horizontal advection, entrainment, and turbulent mixing significantly contribute to the heat budget east of 3°W because of the very thin mixed layer. The upper layers of the north CLR might also be impacted by vertical mixing induced by the intense current vertical shear between the South Equatorial Current, flowing westward at the surface, and the subsurface eastward Equatorial Under-Current. In addition to local forcing, the area is also under the influence of the arrival of equatorial Kelvin waves from West and their reflection, once reaching the African coast, poleward as coastally trapped waves and westward as Rossby waves (Moore, 1968; McCreary, 1976; Moore and Philander, 1977). The principal source of the equatorial Kelvin waves has been usually related to the western equatorial zonal wind changes during late boreal winter to early summer (e.g.; Philander, 1990). In order to better understand the triggered mechanism of Kelvin waves generation which conditions the mixed layer properties in the CLR, another purpose of this study is thus to identify the atmospheric conditions coinciding with the Kelvin waves generation in the West of the basin during winter 2005 and 2006.

Several studies (*e.g.* Okumura and Xie, 2004; Caniaux et al., 2011; Nguyen et al., 2011; Thorncroft et al., 2011) put into evidence a high correlation between the ACT and the WAM onset in the Sahelian region. Based on an analysis of 27 years of data, Caniaux et al. (2011) identified the year 2005 as the year with the earliest WAM

Ocean Sci. Discuss., https://doi.org/10.5194/os-2017-74
Manuscript under review for journal Ocean Sci.
Discussion started: 4 October 2017

onset date (around 19 May 2005 whereas they define the mean onset date on 23 June +/-8 days). According to Marin et al. (2009), the time shift in the development of the ACT between 2005 and 2006 is related to a particular wind burst event in mid-May 2005. This mid-May 2005 event therefore appears as exerting a strong influence on the WAM. In a second part of the study, we thus focus on this particular wind event that preceded a strong cold event in the far eastern Tropical Atlantic along with an early ACT development. We aim to describe i) the atmospheric and oceanic conditions during this particular event; ii) to what extent it is involved in the WAM system; and iii) which processes make it an exceptional event.

The remainder of the paper is organized as follows. In Sect. 2, the model and observational data used in this study are described. The seasonal and interannual variability of SST, winds, currents, 20° C-isotherm depth and sea surface heat flux in the CLR are analyzed in Sect. 3. The cooling events generated in response to southerly wind bursts and the other forcing mechanisms implied in the CLR are investigated in details for the years 2005 and 2006 in Sect. 4. In Sect. 5, we focus our analysis on the unusual wind burst occurring in mid-May 2005. Finally, the main results are summarized and discussed in Sect. 6.

2. Model and data

The numerical model used in this paper is the Regional Oceanic Modeling System (ROMS) (Shchepetkin and McWilliams, 2005). The model configuration is the same as employed in Herbert et al. (2016), and the following text is derived from there with minor modifications.

ROMS is a three-dimensional free surface, split-explicit ocean model which solves the Navier-Stokes primitive equations following the Boussinesq and hydrostatic approximations. We used the ROMS version developed at the Institut de Recherche pour le Développement (IRD) featuring a two-way nesting capability based on AGRIF (Adaptative Grid Refinement In Fortran) (Debreu et al., 2012). The two-way capability allows interactions between a large-scale (parent) configuration at lower resolution and a regional (child) configuration at high resolution. The ROMSTOOLS package (Penven et al., 2008) is used for the design of the configuration. The model configuration is built following the one performed by Djakouré et al. (2014) over the Tropical Atlantic. The large scale domain extends from 60° W to 15.3° E and from 17° S to 8° N and the nested high resolution zoom focuses between 17° S and 6.6° N and between 10° W and 14.1° E domain. This configuration allows for equatorial Kelvin waves induced by trade wind variations in the western part of the basin to propagate into the Gulf of Guinea and influence the coastal upwelling (Servain et al., 1982; Picaut, 1983). The horizontal grid resolution is 1/5° (i.e. 22 km) for the parent grid and 1/15° (i.e. 7 km) for the child grid (see Herbert et al. (2016), their Fig. 1). This allows an accurate resolution of the mesoscale dynamics since the first baroclinic Rossby radius of deformation ranges from 150 to 230 km in the region (Chelton et al., 1998). The vertical coordinate is discretized into 45 sigma levels with vertical S-coordinate surface and bottom stretching parameters set respectively to theta_s = 6 and theta_b = 0, to keep a sufficient resolution near the surface (Haidvogeland Beckmann, 1999). The vertical S-coordinate Hc parameter, which gives approximately the transition depth between the horizontal surface levels and the bottom terrain following levels, is set to Hc = 10

m. The GEBCO1 (Global Earth Bathymetric Chart of the Oceans) is used for the topography (www.gebco.net). The runoff forcing is provided from Dai and Trenberth's global monthly climatological run-off data set (Dai and Trenberth, 2002). The rivers properties of salinity and temperature are prescribed as annual mean values. One river (Amazon) is prescribed in the parent model while five rivers, that correspond to the major rivers present around the Gulf of Guinea, are prescribed in the child model (Congo, Niger, Ogoou, Sanaga, Volta). At the surface, the model is forced with the surface heat and freshwater fluxes as well as 6 hourly wind stress derived from the Climate Forecast System Reanalysis (CFSR) (horizontal resolution of ¼°x ¼°) (Saha et al., 2010). Our model has three open boundaries (North, South, and West) forced by temperature and salinity fields from the Simple Ocean Data Analyses (SODA) (horizontal resolution of ½°x½°) (Carton et al., 2000a, 2000b; Carton and Giese, 2008). The simulation has been performed on IFREMER Caparmor super-computer and integrated for 30 years from 1979 to 2008 with the outputs averaged every 2 days. A statistical equilibrium is reached after ~10 years of spin-up. Model analyses are based on the 2-days averaged model outputs from year 1998 to year 2008. The model has already been validated successfully with a large set of measurements and climatological data, and more detailed information about the model validations can be found in Herbert et al. (2016).

For SST observations, we use data obtained from measurements made by the Tropical Rainfall Measuring Mission microwave imager (TMI). The dataset is a merged product available at www.remss.com. The SST data have a spatial resolution of ¼° and for the present study the 10 years' time series, from 1 January 1998 to 31 December 2008, obtained as 3-daily field. The important feature of the microwave retrievals is that it can give accurate SST measurements under clouds (Wentz et al., 2000). However, the major limitation to the microwave TMI observations is land contamination which results in biases of the order of 0.6°K within about 100 km from the coast (Gentemann et al., 2010). Thus, in the Optimal Interpolation TMI product the offshore zone with no data extends at approximately 100 km from the coast. This limits to some degree the analysis of near-coastal regions, in particular those dominated by coastal upwelling dynamics.

We also use for this study daily sea surface height (SSH) data, which are available for the period 1993–2012 and maintained by the organization for Archiving, Validation, and Interpretation of Satellite Oceanographic data (AVISO; www.aviso.altimetry.fr). The sea surface height dataset is a merged product of observations from several satellite missions Ssalto/Duacs (Segment Sol multimissions d'ALTimétrie, d'Orbitographie et de localisation précise/Developing Use of Altimetry for Climate Studies) mapped onto a 0.25° Mercator projection grid. All standard corrections have been made to account for atmospheric (wet troposphere, dry troposphere and ionosphere delays) and oceanographic (electromagnetic bias, ocean, load, solid Earth and pole tides) effects. The mean sea surface topography for the period 1993–2012 was removed from the SSH to produce sea surface height anomalies.

In addition, surface pressure data were studied using ECMWF Atmospheric Reanalysis (ERA) for the 20th Century product. The four-hourly data are daily averaged and is available on https://rda.ucar.edu website. The product assimilates surface pressure and marine wind observations.

Ocean Sci. Discuss., https://doi.org/10.5194/os-2017-74
Manuscript under review for journal Ocean Sci.
Discussion started: 4 October 2017

177

178 **3. Seasonal variability of surface conditions in CLR**

179 The purpose of this section is to describe the seasonal atmospheric and ocean surface conditions in the CLR.

180 The seasonal variability of SST, surface winds stress, horizontal current intensity, depth of 20° C-isotherm
181 (hereafter referred to as z20), and the surface net heat flux from monthly averaged model outputs in the CLR for
182 each year from 1998 to 2008 and averaged over the period are shown on Fig. 1. The reliability of the model is
183 also provided by comparing the simulated and the corresponding TMI SST climatological seasonal cycle in the
184 CLR (Fig. 1a). The SST variations display an annual cycle with highest temperature in boreal winter (warm
185 season), when the ITCZ reaches its southernmost position and the trade winds are weakest, and minimum values
186 in boreal summer (cold season), when the trades intensify. The most salient features of the atmospheric and
187 hydrographic fields during May-June are also illustrated on Fig. 1 by May-June averaged maps. Despite a warm
188 bias (~1° C) compared to satellite observations, well known in the eastern tropical Atlantic region (e.g. Zeng et
189 al., 1996; Davey et al., 2002; Deser et al., 2006; Chang et al., 2007; Richter and Xie, 2008), the model pretty
190 well reproduces the satellite SST pattern. The SST May-June average map indicates that the boreal summer SST
191 minimum is related with intensified cool SST around 6°S, in the Congo mouth region. In this region, the coast is
192 oriented parallel to the trade flow which reinforces in boreal summer, thus favorable to coastal upwelling
193 processes. The mean alongshore wind stress during May-June reveals in fact that upwelling conditions are
194 observed over most of the CLR. Wind stress magnitude exhibits a semi-annual variability with a second
195 maximum in October–December and a weakening during July-September season (Fig. 1b). The strengthening of
196 winds in spring is associated with a strengthening of mean current speed, particularly off Cape-Lopez between
197 2° S to 4° S and west of 8° E in May-June (Fig. 1c). The orientation of surface current is mostly westward for
198 the May-June season, while it is northward from October to January (not shown). This general picture of surface
199 circulation is consistent with observations (Merle, 1972; Piton, 1988; Rouault et al., 2009).

200 The region is also characterized by a shallow thermocline which depicts a strong semi-annual cycle (Fig. 1d).
201 The evolution of z20 reveals a thinning of the thermocline during May-July and a thickening up to October-
202 November when it exhibits a minimum.

203 The surface net heat flux exhibits a maximum in winter and a minimum in July (Fig. 1e), following the seasonal
204 cycle of solar shortwave radiations. As visible on the May-June average map, greater heating is found over cool
205 waters, due to weaker heat loss via latent heat flux in these areas.

206 The seasonal cycle is modulated by strong year-to-year variations. The mean SST in the CLR in 2005 cools as
207 early as March from TMI data and April from the model data. SST reaches weaker values than the climatologic
208 ones, as observed by Marin et al. (2009) and Caniaux et al. (2011) west of 4° E. This 2005 cold anomaly is
209 associated with positive wind speed and surface current speed anomaly in April-May (Fig. 1b&c) as well as
210 shallower-than-average thermocline depth. In 2006, SST variations are very close to the climatologic ones.
211

Ocean Sci. Discuss., https://doi.org/10.5194/os-2017-74
Manuscript under review for journal Ocean Sci.
Discussion started: 4 October 2017

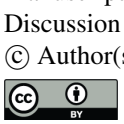

Ocean Science
Discussions
Open Access
EGU

212 Thus, the April-June season in the CLR appears as a transitional period characterized by strong seasonal
213 evolution, primarily governed by the local winds which generate coastal upwelling in Congo mouth region and
214 modulated by the variation of thermocline depth.

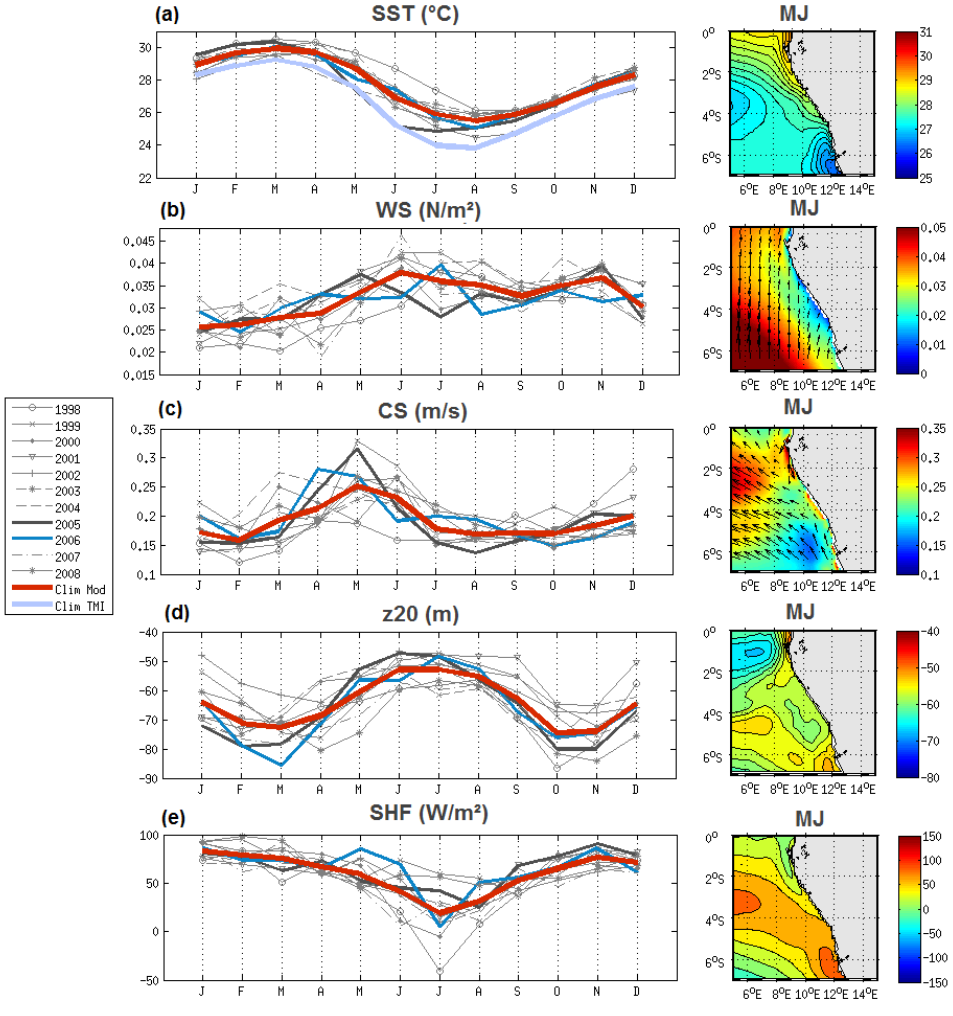

215

216 **Figure 1**: Monthly average of the (a) sea surface temperature (°C); (b) wind stress magnitude ($N.m^{-2}$); (c)
217 horizontal current speed ($m.s^{-1}$); (d) 20° C-isotherm depth anomalies (m); and (e) surface heat flux ($W.m^{-2}$) from
218 January to December from 1998 to 2008 and for the climatology (averaged over 1998-2008) simulated by the
219 model (red curve) and from the observations : monthly average TMI 3-daily SST data (light blue curve in (a));
220 averaged over 5° E-14° E and 7° S-0° S. Right panel: maps of each variable over May-June. For the wind and
221 the surface current, the color field shows the wind stress magnitude and the current speed respectively.

Ocean Sci. Discuss., https://doi.org/10.5194/os-2017-74
Manuscript under review for journal Ocean Sci.
Discussion started: 4 October 2017

222

223 **4. Analyze of cooling events in CLR in 2005 and 2006**

224 In this section, we examine the impact of intraseasonal wind bursts on SST in CLR during the particular years
225 2005 and 2006 (Marin et al., 2009; Caniaux et al., 2011). We propose here to analyze in details the SST
226 conditions in CLR, east of 5° E, for both years.
227
228
229 **4.1 SST variations**

230 In order to delineate the sequence of cooling events, we analyze the SST variations from 2-days averaged model
231 outputs in 2005 and 2006 over the CLR, i.e. between 5° E and 12° E (Fig. 3a&4a). In 2005, the intraseasonal
232 cooling events took place on 22-24 April, 8-12 May, 16-20 May, 26-30 May, 12-16 June and 30 June-2 July,
233 with a temperature drop ranging between -0.2°C to -1.7°C. The cooling events occurred east of 5° E from May
234 to September. They concerned especially the southern equatorial region (around ~3-4° S), except for the
235 strongest events where they reached more northern equatorial regions, especially for the mid-May and late-May
236 2005 events. These latter were associated with an intense meridional SST front between the cold water south of
237 the equator and the warmer water north of the equator, as visible on SST map for 12 May 2005 presented on
238 Fig. 2. We can see cold waters extending along the eastern coast and in ACT region west of 5° W. In the model,
239 cold waters are deflected offshore off Cape-Lopez, due to recursive bias in warm water intrusion toward the
240 south.

241 Besides, model SST fields (Fig. 3a) indicate that the SST minimum (~24° C) in 2005 was reached in July, i.e.
242 one month earlier than in 2006, as also noticed in seasonal variations of SST averaged in the region (Fig. 1a).
243 These results illustrate the important role in the CLR of the succession of quick and intense cooling events in the
244 establishment of persistent cold anomalies, as highlighted by Marin et al. (2009) in the equatorial region.

245

246

Ocean Sci. Discuss., https://doi.org/10.5194/os-2017-74
Manuscript under review for journal Ocean Sci.
Discussion started: 4 October 2017

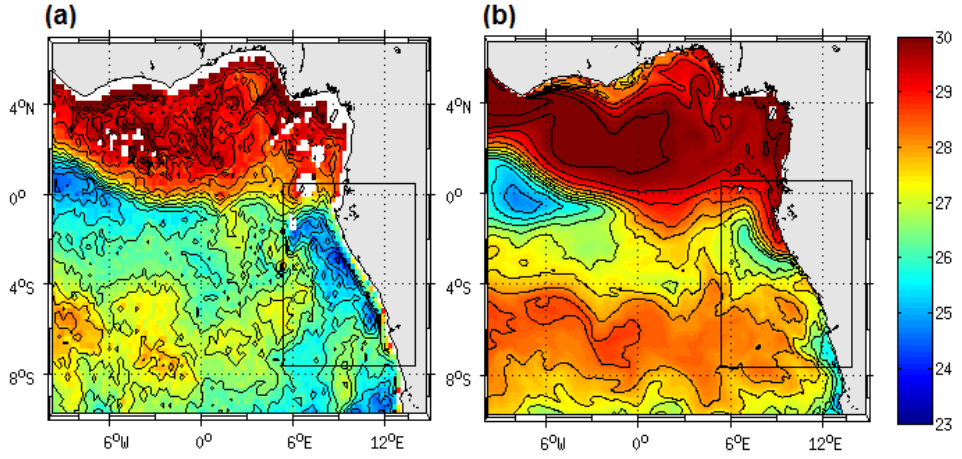

Figure 2: Map of the sea surface temperature (° C) on 12 May 2005 from 3-days average TMI data (a) and from the 2-days average model output (b). Note that for the model it corresponds to 11-12 May average whereas for TMI data it is 10-11-12 May average. The black square indicates the Cape-Lopez region (called 'CLR').

4.2 Forcing mechanisms

4.2.1. Local forcing

To examine the local forcing mechanisms responsible for the observed cooling events in CLR, the intraseasonal variations of wind stress magnitude anomalies are examined and compared in 2005 and 2006 (Fig. 3b & 4b).

In 2005, successive periods of 6-16 days wind intensification occurred from late-March to late-May. The main cooling events described above are associated with positive wind stress speed anomalies occurring on 12-24 April, 2-6, 12-16 & 24-28 May, 8-12 & 28 June, with a maximum for the 12-16 May event peaking on 14 May (at ~0.03 $N.m^{-2}$). Another period of wind intensification is evidenced in late March – early April but it did not generate significant cooling despite comparable or even higher wind intensity than following wind events. In 2006, periods of wind intensification were slightly shorter than in 2005 and extended from mid-March to mid-May, interrupted by periods of negative wind anomalies. The main wind events occurred in 16-18 March, 2-4 & 16-24 April, 4-6 & 12-18 May, with maximum wind stress magnitude anomaly in 16-24 April. Also, the wind event in late April 2006 did not generate a surface cooling as strong as the mid-May 2006 one, despite higher wind stress magnitude anomalies. To depict the subsurface conditions during cooling events in CLR for both years, anomalies of the 20° C-isotherm depth averaged from 5° E to 12° E are presented on Fig. 3c & 4c. They indicate strong correlation with SST anomalies on intraseasonal time scale with maximum values (up to + 25 m) observed during the 14 May 2005 event. In early April 2005 and before the late-April 2006, the thermocline was deeper, that can explain why wind intensification did not generate a surface cooling at these times. Indeed, at the

Ocean Sci. Discuss., https://doi.org/10.5194/os-2017-74
Manuscript under review for journal Ocean Sci.
Discussion started: 4 October 2017

time of the strong 16-24 April 2006 wind event, the z20 anomalies was weaker south of the equator than during the 14-16 May 2005 event, making the SST less reactive to comparable wind intensification. The same feature is observed in early May 2006, when the z20 anomalies indicate deeper thermocline south of the equator around 4° S than a few days later. Besides, the thermocline appeared shallower south of the equator in 2005 than in 2006, in agreement with the difference of the cooling intensity observed between the two years.

The Ekman pumping velocity w_e averaged along 3-4° S is shown on Fig. 3d. It is correlated with wind intensity, with maximum around 8°E at the dates of the 2005 and 2006 events, in agreement with the cooling events identified mostly around 3-4°S (Fig. 3a & 4a). The maximum upward velocity sometimes extended west of 8° E, as during April 2005 and June 2006 events.

Another process that may contribute to the cooling in the upper layer is the vertical mixing due to intense vertical shear of the zonal current. The maximum of the zonal current vertical shear fields in CLR, averaged between 5° and 12° E for 2005 and 2006 (Fig. 3e & 4e), exhibited intensification south of the equator, centered around 3-4° S. Weaker intensification also occurred occasionally at the equator (located around 80 m depth between the westward surface South Equatorial Current – SEC – and the eastward subsurface Equatorial Under-Current). Around 3-4° S, the vertical shear was driven by the SEC, reinforced by prevailing southerly winds events through Ekman transport. It thus occurred at the date of wind events previously identified for 2005 and 2006, with stronger vertical shear occurring in early May 2005. The intensity of the maximum of vertical shear during the events was quite similar between 2005 and 2006. The main difference lied in their meridional extent, related to the meridional extent of the strengthened southerly winds which reached equatorial region during the May 2005 events (not shown). We can also notice that for comparable wind intensification, the spring and summer wind events were not associated with comparable intensity of vertical shear. The meridional wind component favorable to westward Ekman transport was actually stronger during April and May events than during summer ones (not shown).

The heat content within the mixed layer is also impacted by the sea surface heat fluxes. The net heat fluxes averaged between 5° E and 12° E are shown on Fig. 3f & 4f for 2005 and 2006 respectively. They indicate a net heating (~ 50-100 $W.m^{-2}$) over the 2° S - 5° S latitude band, where the SST cooling was strongest, suggesting other mechanisms involved. However, we notice some particular events during which the net heat flux was negative over most of the region. The strongest net cooling (-30 $W.m^{-2}$) occurred during the 26-28 May 2005 event. It was mainly due to a sudden decrease of incoming surface short wave radiation (drop of about 140 $W.m^{-2}$ between 22 and 28 May; not shown) suggesting increased cloud cover.

Ocean Sci. Discuss., https://doi.org/10.5194/os-2017-74
Manuscript under review for journal Ocean Sci.
Discussion started: 4 October 2017

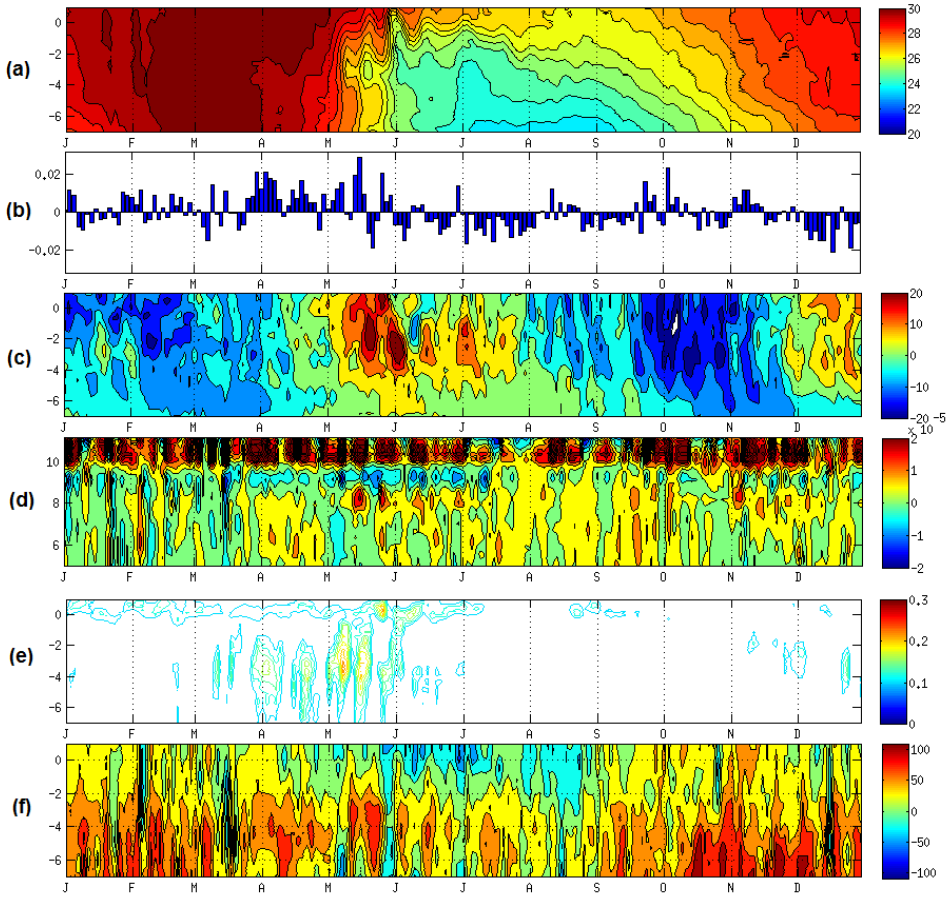

Figure 3: (a) Time-latitude diagram, from 7° S to 1° N, of the sea surface temperature (in ° C) averaged between 5° E and 12° E; (b) Time evolution of the wind stress amplitude anomalies ($N.m^{-2}$) averaged between 5° E and 12° E and between 3° S and 0° S; (c) Latitude-time diagram of the 20° C-isotherm depth anomalies (m) averaged between 5° E and 12° E; (d) Longitude-time diagram of Ekman Pumping anomalies ($m.s^{-1}$) averaged between 3° S and 4° S; (e) Latitude-time diagram of the maximum of the zonal current vertical shear ($m.s^{-1}$) averaged between 5° E and 12° E (only the values > $0.1 m.s^{-1}$ are plotted) ; (f) Latitude-time diagram of the net heat flux ($W.m^{-2}$) averaged between 5° E and 12° E; from 1st Jan. to 31 Dec. 2005.

Ocean Sci. Discuss., https://doi.org/10.5194/os-2017-74
Manuscript under review for journal Ocean Sci.
Discussion started: 4 October 2017

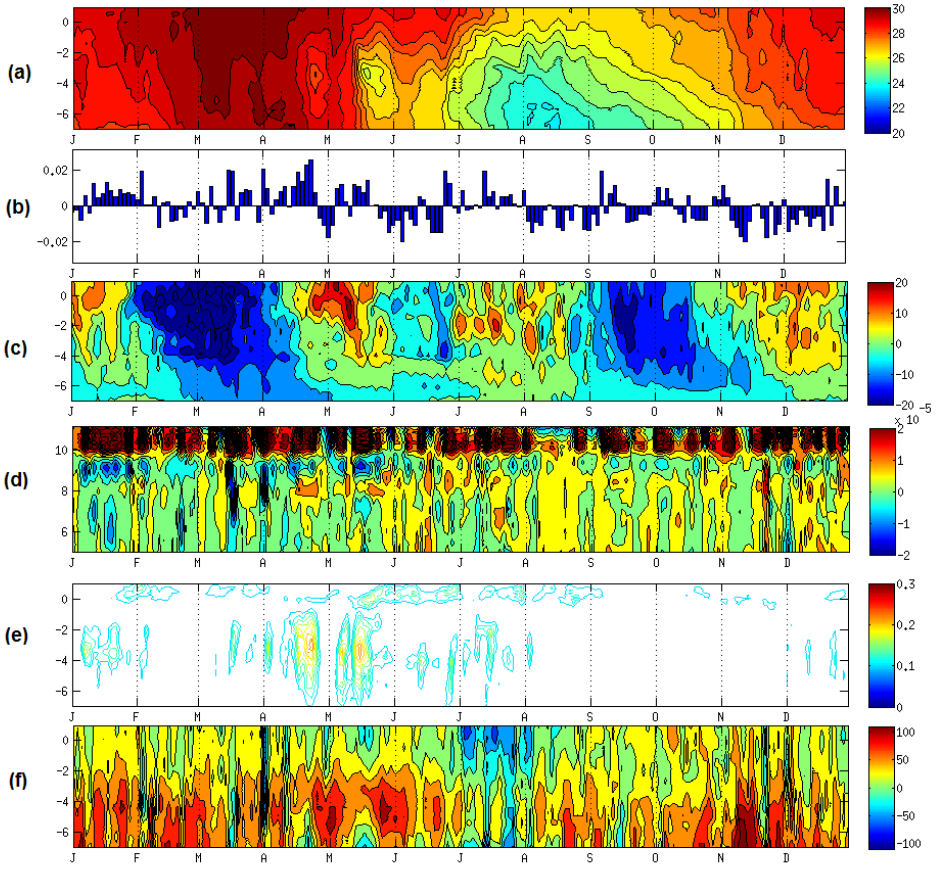

312

313 **Figure 4**: Same than Figure 3 but for 2006.

314

315 **4.2.2. Remote forcing**

316 **a. Highlighting of Kelvin wave propagation**

317 As previously shown, the time of occurrence of the cold events in the CLR coincides with steeper thermocline
318 slope which allows a mixed layer temperature to be more reactive to surface forcing. Indeed, because of its
319 proximity to the equator, the thermocline in CLR is affected by the arrival of equatorial waves, initiated in the
320 west part of the basin. Pairs of alternate downwelling and upwelling Kelvin waves occur usually in February-
321 March, July-September and October-November. Upon impingement with the eastern boundary, the incoming
322 equatorial Kelvin wave excites westward-propagating Rossby waves and poleward-propagating coastal Kelvin
323 waves (Moore, 1968; Moore and Philander, 1977; Illig et al., 2004; Schouten et al., 2005; Polo et al., 2008). The

Ocean Sci. Discuss., https://doi.org/10.5194/os-2017-74
Manuscript under review for journal Ocean Sci.
Discussion started: 4 October 2017

20° C-isotherm depth anomalies along the equator and along 9°E are presented on Fig. 5 and clearly evidence large positive anomalies indicating shallower-than-average thermocline, propagating eastward along the equator and then southeastward for both years. The eastward propagation of Kelvin wave along the equator and southeastward along the coast is also well visible in the basin-wide SSH anomalies (Fig. 6) with a phase velocity of about 1.1-1.3m.s^{-1}, which fits well in the range between the second and third baroclinic equatorial Kelvin wave modes. The upwelling wave is in fact detectable by negative SSH anomalies, associated with shallower-than-average thermocline. In 2005, negative (positive) SSH (z20) anomalies occurred in the West in early April and in mid-May, whereas they occurred around late-March and early May in 2006. The first Kelvin wave thus reached the CLR slightly earlier in 2006 than 2005, at the beginning of May.

Thus, the intensity of the cold events observed in spring and summer 2005 and 2006 resulted from both the basin preconditioning by remotely forced shoaling of the thermocline, local mixing and upwelling processes in response to strong southerly local winds, as well as heat flux variations. In 2005, stronger wind intensification and favorably preconditioned oceanic subsurface conditions, made the coupling between surface and subsurface ocean processes more efficient than in 2006, resulting in stronger cooling.

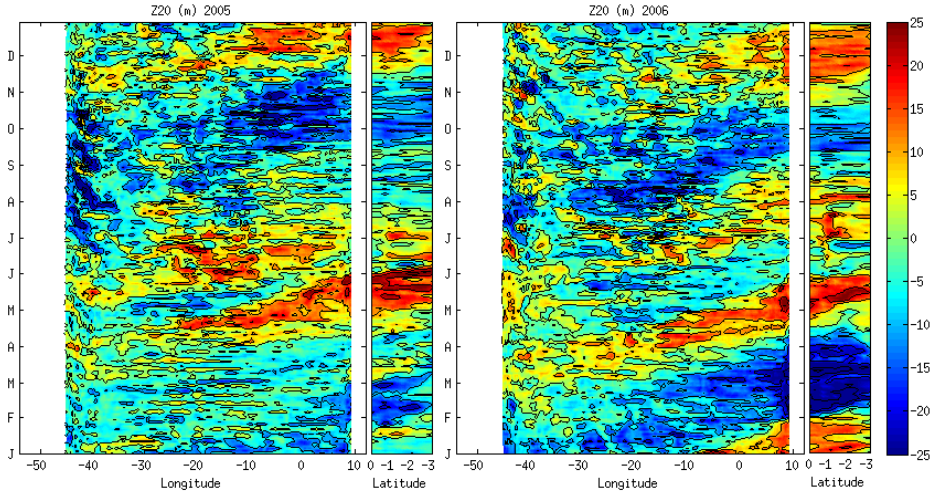

Figure 5: Time evolution of the 20° C-isotherm depth anomalies (m) along the equator (between 54° W and 12° E) and along 9° E (between the equator and 3° S) for 2005 (left) and 2006 (right).

Ocean Sci. Discuss., https://doi.org/10.5194/os-2017-74
Manuscript under review for journal Ocean Sci.
Discussion started: 4 October 2017

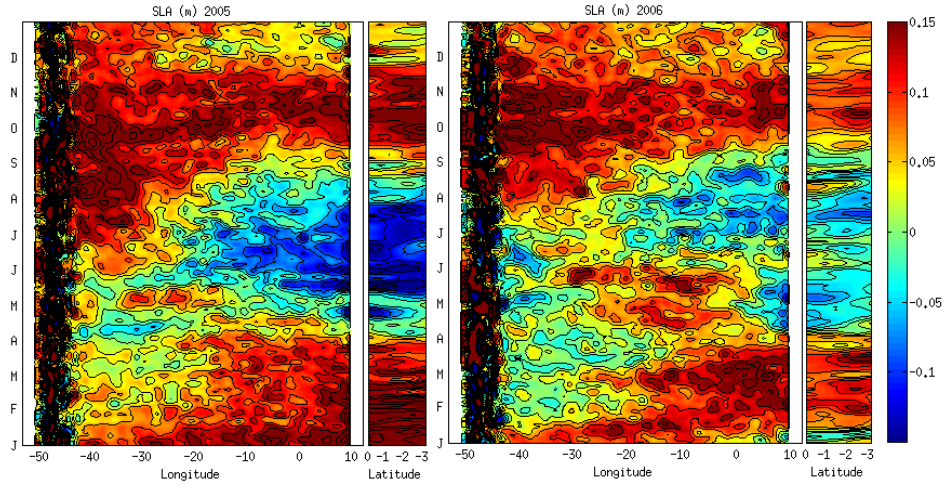

Figure 6: Time evolution of the sea level anomaly (m) along the equator (between 54° W and 12° E) and along 9° E (between the equator and 3° S) for 2005 (left), and 2006 (right) from AVISO data.

b. Kelvin wave generation and coinciding atmospheric conditions in the West

In order to identify the wind activity which accompanies the excitation of Kelvin upwelling waves in winter 2005 and 2006 in the west part of the basin, we analyze the position of the ITCZ (averaged over 50° W-35° W) identified as the latitude where the meridional wind stress goes to zero (Fig. 7a). The anomaly of zonal and meridional components of the wind stress (Fig. 7b&c), the wind stress curl anomaly (Fig. 7d), as well as the z20 and SSH anomalies (Fig. 7e&f), averaged in the equatorial band (over 1° S and 1° N), are also presented. For the zonal wind stress, the frequencies > 1 month are removed by a low-pass filtering and superimposed with the anomalies (red curve on Fig. 7c). Many authors suggest that the source of the equatorial Kelvin wave is mainly related to a sudden change of the western equatorial zonal wind (e.g. Picaut, 1983; Philander, 1990): a symmetric westerly (easterly) wind burst along the equator will generate Ekman convergence (divergence) and thus force downwelling (upwelling) anomalies which then propagate eastward as a Kelvin wave (Battisti, 1988; Giese and Harrison, 1990). In 2005, shallower-than-average thermocline, evidenced by positive (negative) z20 (SSH) anomalies, occurred in the end of March-beginning of April in the west part of the basin (Fig. 7e&f). The meridional and zonal wind stress anomalies indicate that the maximum of thermocline slope anomaly was associated with a strengthening of northeast trades followed by a strengthening of southeast trades from either side on the equator. At the equator, we notice indeed a sudden reversing of meridional winds which turned southward on 27-28 March 2005 related to an abrupt southward displacement of the ITCZ which was then found south of the equator in the west part of the basin (Fig. 7a&b). The ITCZ returned its initial position four days later followed by a strengthening of easterlies which persisted for ~20 days (Fig. 7c). Climatologically, the

Ocean Sci. Discuss., https://doi.org/10.5194/os-2017-74
Manuscript under review for journal Ocean Sci.
Discussion started: 4 October 2017

latitudinal position of the ITCZ varies from a minimum close to the equator in boreal spring (March-May) in the west to a maximum extension of 10°N – 15°N in late boreal summer (August) in the east. Positive (negative) wind stress curl is found north (south) of the ITCZ. When the ITCZ is north of the equator, it induces upward (downward) Ekman pumping to the north (south) of the ITCZ. Thus, the southward shift of the ITCZ on 27-28 March 2005 accompanied with strong northerlies led to negative anomaly of wind stress curl south of the equator resulting in upward Ekman pumping. Results show indeed a strong negative anomaly on 22-26 March 2005 associated with the southward shift of the ITCZ just before the upwelling signal, initiated on 28 March. These changes contributed to a rise in the oceanic thermocline with a time lag of some days (Fig. 7e&f). The upwelling signal might then be reinforced by the symmetric easterly wind which concerned a large part of the western basin. Besides, we identify on Fig. 6d another peak of negative wind stress curl anomaly on 6-8 May 2005, more sudden than the previous winter one. It was associated with positive (negative) z20 (SSH) anomaly indicator of a thermocline rise initiated on 6 May 2005 in the west of the basin and which propagated eastward along the equator. The zonal wind stress anomalies (Fig. 6b) also indicate an easterly wind strengthening initiated in the beginning of May, which a maximum on 8-10 May, just after the minimum of wind stress curl.

In 2006, the upwelling Kelvin wave is identified in the first half of March in the west part of the basin (Fig. 7e&f). The coinciding atmospheric conditions were slightly different than the ones identified in 2005. In winter, the position of the ITCZ had a more southern position in 2006 than in 2005. It crossed the equator during a longer period (about 10 days from ~ Feb. 10 2006), reaching minimum latitude on 22-24 February. This location south of the equator induced a negative wind stress curl anomaly (Fig. 7d). As in 2005, the reversion of the meridional wind at the equator was followed by a strengthening of westward component of the wind stress few days after, which lasted for about ten days (Fig. 6c); however, it was of a lesser magnitude compared to 2005 and only concerned the westernmost part of the basin. In addition, the negative zonal wind anomaly concerned mainly the northeasterlies rather than the southesterlies, leading to an anti-symmetric meridional wind pattern as well as symmetric zonal wind pattern on either side on the equator (not shown). These wind patterns were expected to generate Ekman convergence at the Equator and thus to reinforce the observed upwelling anomalies.

Thus, for both years, Kelvin upwelling wave occurred in the west while easterly winds were strengthened from either side of the equator after the ITCZ reached its southernmost location. This latter was observed one month earlier in 2006 than in 2005, and was associated with a negative wind stress curl anomaly. In winter 2005, the ITCZ was found south of the equator after a very sudden southward shift and was followed by strong easterlies during ~20 days, while in winter 2006, the ITCZ was found closer to the equator less sharply and during a longer period, followed by weaker easterlies compared to 2005.

Ocean Sci. Discuss., https://doi.org/10.5194/os-2017-74
Manuscript under review for journal Ocean Sci.
Discussion started: 4 October 2017

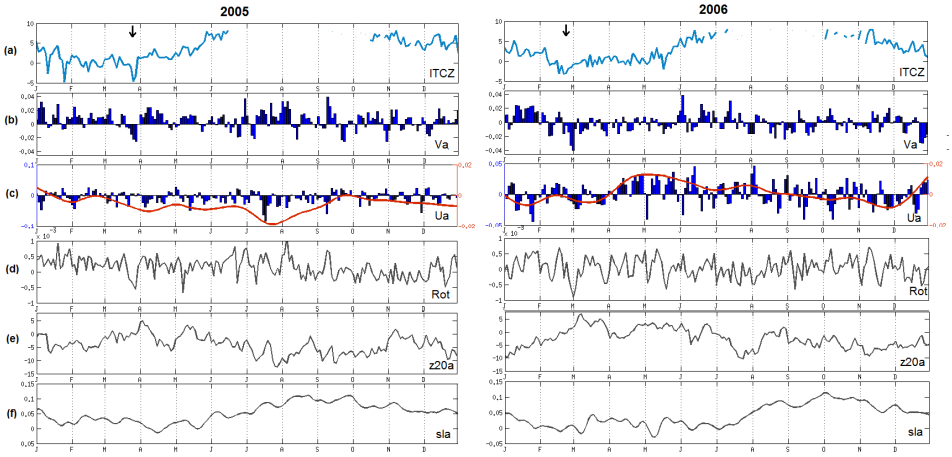

399

400 **Figure 7**: Time evolution, from 2-days averaged model outputs, of (a) the position (in latitude, between 5° S
401 and 10° N) where the meridional wind stress value equal zero (indicator of the position of the ITCZ), over Jan-
402 Dec 2005 (left) and Jan-Dec 2006 (right); (b) the meridional wind stress anomalies ($N.m^{-2}$) averaged between
403 50° W and 35° W and between 1° S and 1° N; (c) same as (b) but for zonal wind stress anomalies ($N.m^{-2}$) (in
404 blue). The red curve is after the frequencies > 1 month are removed by a low-pass filtering; (d) the wind stress
405 curl anomalies ($N.m^{-2}$) ; (e) the 20° C isotherm depth anomalies (m); (f) the sea level anomalies (m). The black
406 arrow in (a) indicates the southward shift of the ITCZ before the excitation of the Kevin wave (see text).

407

408 **4.3. Westward extension of the CLR cooling**

409 In the east, the cooling generated by southerly wind bursts in the CLR then progressively extended westward to
410 connect with the southern boundary of the equatorial ACT. This phenomenon was more obvious in 2005 when
411 the cooling which first concerned coastal area extended further offshore a few days after the two strong events
412 occurring in the second half of May. To evidence the effect of these events on SST, maps of SST anomalies and
413 wind stress monthly anomalies averaged over May 2005 and over the weeks before the strong events (from 1 to
414 10 May) are presented on Fig. 8. The results illustrate an enhancement after 10 May of the cooling in the east
415 associated with southerly wind intensification and an extension of the cooling especially south of the equator up
416 to 20°W.

417

418

419

420

Ocean Sci. Discuss., https://doi.org/10.5194/os-2017-74
Manuscript under review for journal Ocean Sci.
Discussion started: 4 October 2017

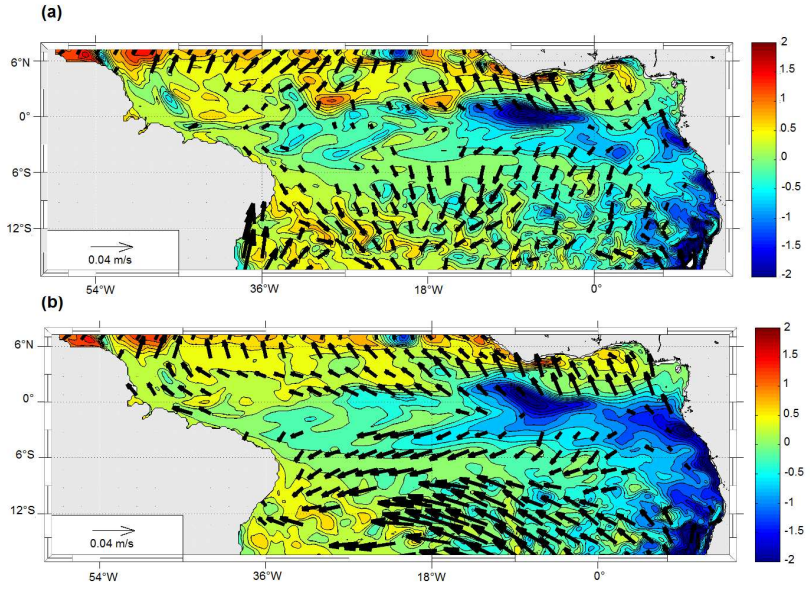

Figure 8: (a) Sea surface temperature anomalies (° C; color) superimposed with wind stress intensity anomalies (arrows) averaged over May 2005. Only the values > 0.02m.s^{-1} are plotted; (b) same but averaged between 1 May and 10 May 2005 (b)

To better understand the oceanic processes implied in this cooling extension, we examined the z20 anomalies, SSH anomalies and zonal velocities along 3° S (Fig. 9 b-d). They reveal that the cooling westward extension was associated with a westward propagation of a steeper thermocline and negative SSH anomalies from the African coast up to 5°-10° W combined with enhanced surface westward current fluctuations at the dates of the successive events from April-June. The fluctuations of the westward surface current occurring off Gabon with periods of ~8-10 days were related to the strengthening of southerly winds during the wind bursts at the same periods (Fig. 3b & 4b). The surface current in this area is part of the westward SEC which is known to intensify during the cold season (Okumura and Xie, 2006). Our study implies shorter time scales than seasonal scale but the intensification of the SEC during wind bursts through Ekman transport processes might contribute to the westward extension of the cooling by advection of cold eastern upwelled water. This is in agreement with DeCoëtlogon et al. (2010) who found from model results that at short time scale (a few days), more than half of the cold SST anomaly around the equatorial cooling could be explained by horizontal oceanic advection controlled by the wind with a lag of a few days. In addition, the z20 and SSH show respectively negative and positive anomalies propagating westward at 3° S (Fig. 9), initiated from the coast with a propagating speed of around 10 cm.s^{-1}, which is very close to the phase speed of Rossby waves. Indeed, the excitation of the westward waves at the coast coincided with the arrival of Kelvin waves (see Fig. 5) suggesting the possibility of Kelvin wave's reflection processes into symmetrical westward propagating Rossby waves. A westward

Ocean Sci. Discuss., https://doi.org/10.5194/os-2017-74
Manuscript under review for journal Ocean Sci.
Discussion started: 4 October 2017

propagation of z20 and SSH anomalies, although less obvious, was presently also identified at 3° N (not shown). In 2006, no similar wave generation process is observed (not shown). In 2005, the locally wind-forced component of the wave might reinforce the remote part of the reflected wave signal at the coast by the sea level slope which balanced the strengthening of alongshore winds blowing during the mid-May and late-May events. The quantitative and respective contributions of local and remote wind forcing to this wave is out of the aim of this study and would require further analysis.

Thus, the combined effects of westward surface currents (via advection and vertical mixing through horizontal current vertical shear), local wind influences (via vertical mixing) and wave westward propagation, resulted in the extension of cold upwelled water from the eastern coast to near 20° W.

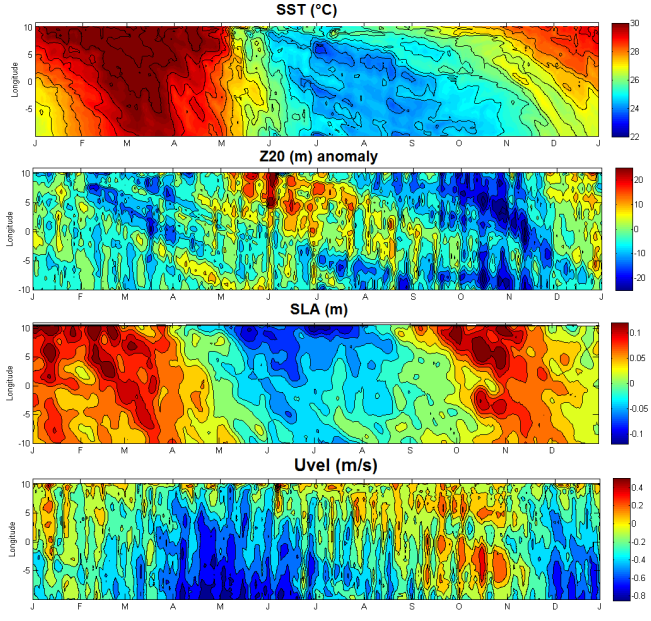

Figure 9: Time-longitude diagrams at 3° S between 10° W and 10° E, and from 2-days averaged model outputs from January to December 2005, of (from top to bottom) i) the sea surface temperature (° C); ii) the 20° C isotherm-depth anomalies (m); iii) the sea level anomalies from AVISO data (m); and iv) the zonal component of surface velocity ($m.s^{-1}$).

5. Focus on the mid-May 2005 event

We have previously identified five main cold events in 2005 (22-24 April, 8-12 May, 16-20 May, 26-30 May and 14-18 June), characterized by a temperature drop ranging from -0.2° C to -1.7° C in the model. Analysis of

Ocean Sci. Discuss., https://doi.org/10.5194/os-2017-74
Manuscript under review for journal Ocean Sci.
Discussion started: 4 October 2017

wind stress magnitude has revealed that each event is associated with strengthening of equatorward winds, especially during the 14-16 May event when the wind stress magnitude anomaly averaged over the CLR is the strongest one. This particular event has been found to be responsible for the sudden and intense SST cooling in the eastern equatorial Atlantic and identified as part of manifestation of temporal variability of the St. Helena Anticyclone (Marin et al., 2009). In this section, we focus on this mid-May event, to better understand the processes in play during this unusual event.

5.1 Atmospheric conditions

5.1.1 Wind and surface atmospheric pressure

The spatial distribution of the mid-May 2005 wind event can be inferred from Fig. 10 where anomalous CFSR wind speed fields superimposed with daily precipitation fields, surface pressure, wind speed curl, and downward shortwave radiation, are presented from 13 May to 17 May. The event was characterized by intense southeasterly wind anomalies east of 15° W and from 30°S to the equator from 13-14 May, concomitant with a strengthening of the easterlies west of 30° W between 30° and 15° S (Fig. 10a). The wind anomaly extended then westward up to 15-16 May when the maximum was located in the western part of the basin off northeastern Brazilian coast. Simultaneously, a strengthening of southerly winds occurred north of the equator in the Gulf of Guinea. The anomalous strong winds during the event were associated with anomalous high pressure core of the Saint Helena Anticyclone, especially on 13-14 May, also associated with particularly low pressure under the ITCZ.

Ocean Sci. Discuss., https://doi.org/10.5194/os-2017-74
Manuscript under review for journal Ocean Sci.
Discussion started: 4 October 2017

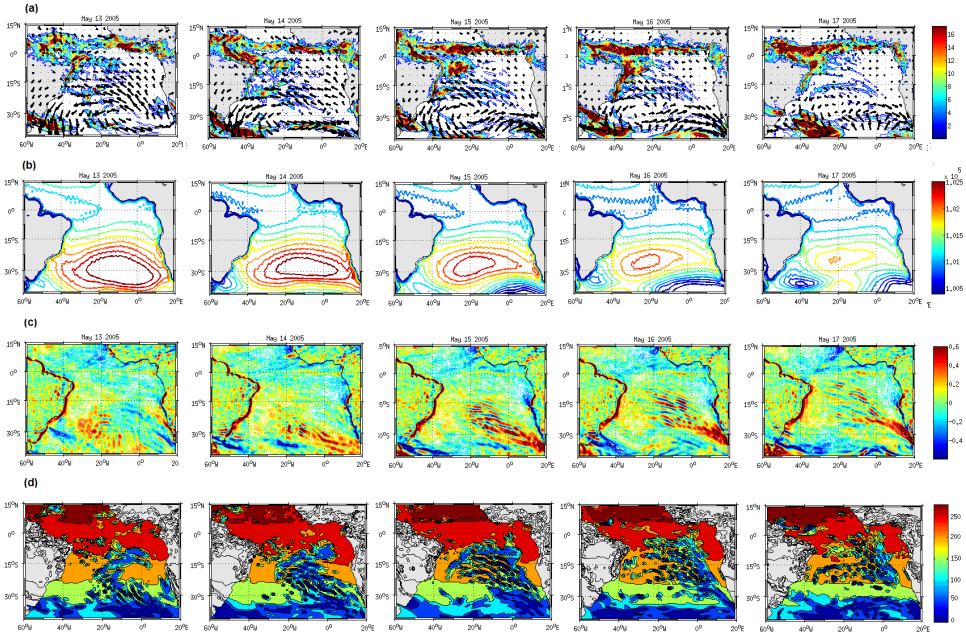

Figure 10: Daily-averaged, from 13 May to 17 May 2005 (left to right panels), of (a) precipitation rate (kg.m^{-2}/day) (color field) superimposed with wind speed anomalies (vectors) (m.s^{-1}) from CFSR fields; (b) surface pressure (hPa) from ERA-20C reanalysis; (c) wind speed curl (m.s^{-1}) computed from CFSR wind speed fields; and (d) downward short-wave radiation (W.m^{-2}) from CFSR fields.

5.1.2 Precipitation

The maps of precipitation rate during the event (Fig. 10a) display a band of heavy precipitation (9-17 kg.m^{-2}/day) between 5° - 9° N and off northeast Brazil from the coast to 15° W and from 10° S to 3° S. The maximum precipitation rate in this region occurred on 15-16 May concomitant with the easterly winds strengthening. This convective zone, located between the ITCZ north of the equator and the South Atlantic Convergence Zone (SACZ) in southern tropics, is the Southern Intertropical Convergence Zone (SICZ) (Grodsky and Carton, 2003). This zone forms usually later, by June-August, when the southern branch of the convection separates from the ITCZ which moves north of the equator. Grodsky and Carton (2003) showed that this rainfall pattern appears closely linked to the seasonal change in SST difference between the ACT region (which they defined between 15° W – 5° W, 2° S – 2° N) and the SITCZ region (25° W - 20° W, 10° S - 3° S). They argued that the seasonal appearance of the ACT along the equator sets up pressure gradients within the boundary layer that induce wind convergence in the SITCZ region. Based on Grodsky and Carton (2003) results, the unusually

rainfall conditions during mid-May event might thus be explained by strong SST gradient between the two regions caused by unusually early cooling in the ACT region at this time of the year.

5.1.3 Generation of atmospheric gravity wave

The precipitation fields during the mid-May event (Fig. 10a) also evidence rainfall pattern typical of atmospheric gravity wave train characterized by a horizontal wave length ~500 km and initiated by a front system (forming the northern boundary of a low pressure system) which developed around 17° S on 14 May and traveled northeastward until 17 May. The rainfall train was associated with oscillatory wind stress curl train alternating between positive and negative anomalies (Fig. 10c) as well as alternating downward shortwave radiation minimum (Fig. 10d) associated with the wave clouds. Gravity waves are known to play an important role in transporting the momentum and energy through long distances (Fritts, 1984). Here, they would be a way to carry momentum and energy from South Atlantic to the equator during the strong event. To estimate the effect of the passage of the wave on SST, the SST TMI fields have been analyzed. Given the time resolution of the dataset (3-days averaged) a propagating train in SST fields cannot be highlighted; instead, 3-daily TMI SST averaged (available east of 10° W) differences, as well as 3-daily averaged downward shortwave radiation (hereafter DSWR) fields differences, between 13-14-15 May averaged and 10-11-12 May averaged and between 16-17-18 May averaged and 13-14-15 May averaged. Results indicate a good correlation between the two fields, suggesting a northeastward propagation of the cooling associated to northeastward propagation of the DSWR minimum associated with the displacement of the atmospheric gravity wave. A cooling first occurred south of 24° S associated with DSWR minimum, and then reached more northern region concomitant with the northward migration of DSWR. Thus, these results suggest that the arrival of atmospheric gravity wave initiated in South Atlantic following atmospheric disturbance would contribute to the cooling observed in the Gulf of Guinea at the time of the mid-May event.

Ocean Sci. Discuss., https://doi.org/10.5194/os-2017-74
Manuscript under review for journal Ocean Sci.
Discussion started: 4 October 2017

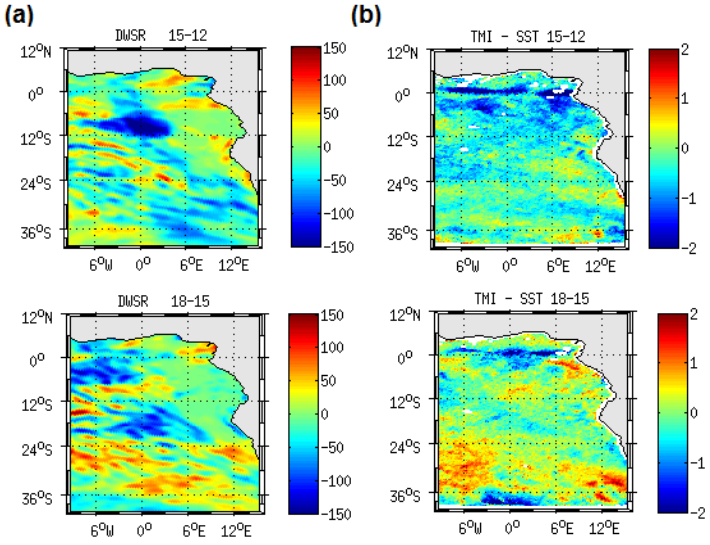

Figure 11: Three daily-averaged differences, between 10° W and 15° E and between 40° S and 12° N from 15-12 May and 18-15 May 2005 (the dates indicated in the titles correspond to the last day taken into account for the calculation of the average. e.g.: 'SST 15-12' corresponds to the difference between the mean of SST over 13-14-15 May and over 10-11-12 May) of downward short-wave radiation ($W.m^{-2}$) from CFSR fields (a); and SST from TMI data (b);

5.2 A decisive event for coastal monsoon onset

In order to analyze the air-sea pattern in the northern Gulf of Guinea during May-June 2005, we show on Fig. 12 the wind stress magnitude, precipitation rate, and SST fields averaged from 10° W to 6° W. The wind strengthening appeared first south of the equator on 12-16 May and then north of the equator from 14-18 May. It was associated with strong rainfall extending southward up to 2° N. Equatorial cooling occurred 4 days after the event and slowed down the overlying winds by feedback mechanisms. The winds north of the equator then remained stronger than in the ACT region and strengthened again north of the Equator on 22-28 May together with precipitation maximum pushed northward (around 5° N) after the event.

Thus, this mid-May event appears as the "decisive event" which triggered the abrupt transition between the two wind patterns in the northern Gulf of Guinea, when the wind north of the equator became and remained stronger than south of the equator. It occurred 15 days earlier than the average date (31 May) identified by Leduc-Leballeur et al. (2013) over 2000-2009 period. According to these authors, the time of occurrence of this phenomenon would be related with the strength of anomalous moisture flux. They explain that in April-May the low atmospheric local circulation is present only during an equatorial SST cooling and surface wind

Ocean Sci. Discuss., https://doi.org/10.5194/os-2017-74
Manuscript under review for journal Ocean Sci.
Discussion started: 4 October 2017

546 strengthening north of the equator, both generated by a southerly wind burst, before disappearing until the next
547 wind burst. In June-July the low atmospheric local circulation is then always present and intensified by the wind
548 bursts. Thus, the establishment of an abrupt seasonal transition event as observed in 2005, occurring much
549 earlier than the reference date, supposed anomalously strong equatorial cooling caused by unusual strong
550 southerly winds which allowed, through air-sea interactions mechanisms, to trigger the deep atmospheric
551 convection in the Gulf of Guinea at a self sustaining level.
552

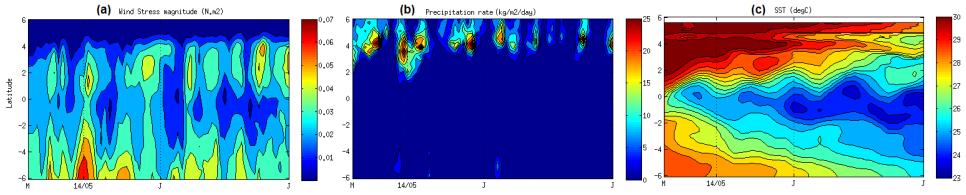

553
554 **Figure 12**: Time evolution, in May and June 2005 between 6° S and 6° N and averaged between 10° W and 6°
555 W, of the (a) daily averaged wind stress magnitude ($N.m^{-2}$) computed from CFSR wind speed fields ; (b) daily
556 averaged precipitation rate ($kg.m^{-2}$/day) from CFSR fields and (c) 2-daily averaged SST (° C) fields, from the
557 forced model.

558

559 **5.3. Why the mid-May 2005 event was so singular?**

560

561 To better understand which makes the particularity of the mid-May 2005 event, the atmospheric and oceanic
562 conditions (wind stress magnitude, short-wave radiation flux (hereafter RADSW), z20, SST, and meridional
563 SST gradient) averaged over the 10° W-6° W region and between 15° S to 5° N during April-May are analyzed
564 along the 1998-2008 period (Fig. 13). The wind stress magnitude during mid-May event appears to be one of the
565 strongest over the whole 1998-2008 period. These strong wind conditions are usually met later in late boreal
566 spring or summer, when the St. Helena Anticyclone strengthens and shifts northward toward the warm
567 hemisphere. The wind intensification in mid-May 2005 was associated with particularly weak RADSW from
568 South Atlantic to the northern equatorial region, suggesting cloud albedo effect during the event which tended to
569 cool the mixed layer. We can notice that the April-May 2005 period was characterized by the weakest mean
570 RADSW.
571 In addition, at the time of the event, the surface waters were already cooled by previous wind bursts (e.g. 20
572 April and 8 May). The SST response to the mid-May event occurred 4-6 days later, inducing the weakest
573 equatorial SST values for April-May season over the whole 1998-2008 period. The cooling also caused an
574 enhanced SST front around 1° N, as shown on Fig. 13 (bottom panel), which was found to be the earliest and
575 strongest one over the 1998-2008 period. This meridional SST gradient was responsible for the wind surface
576 intensification north of the equator (Fig. 12 and 13a) through air-sea interaction mechanisms as described by
577 Leduc-Leballeur et al. (2011). Another SST gradient maximum is found at the end of May 1998 but it was not
578 extended as eastward than during the mid-May 2005 event (not shown).

Ocean Sci. Discuss., https://doi.org/10.5194/os-2017-74
Manuscript under review for journal Ocean Sci.
Discussion started: 4 October 2017

When the wind burst occurred on 14 May 2005, the 20°C-isotherm depth in the area was shallow south of the equator and slightly deeper at the equator (Fig. 13c). The thermocline shoaling associated with the Kelvin wave appeared in fact a few days earlier providing favorable subsurface conditions which made the SST response to previous wind bursts (20 April and 8 May) more effective. At the time of the mid-May event, the wave already reached more eastern areas, as shown in previous sections.

The mid-May 2005 event was also characterized by a particularly low surface pressure under the ITCZ, as shown on Fig. 14a which displays the surface pressure north of the equator averaged between 45° W and 20° W for April-May over the 1998-2008 period. The pressure fall during the mid-May 2005 event appeared as the lowest in May over the whole decade. It coincided with particularly high surface pressures in St. Helena Anticyclone region 4 days earlier (Fig. 14b). The meridional surface pressure gradient during the event is thus found to be the strongest over 1998-2008 period (Fig. 14c). That suggests strong Hadley circulation intensity during the mid-May event and therefore strong anomalous equatorward moisture flux, allowing the deep atmospheric convection in the Gulf of Guinea to be triggered at a self-sustaining level, as previously described in Sect. 5.2.

Thus, the particularity of the mid-May 2005 event mainly lies in the i) anomalous atmospheric conditions related to anomalous strong St. Helena Anticyclone perturbation; ii) cooling initiated by the succession of previous wind bursts; and iii) favorable subsurface local ocean conditions preconditioned by equatorial waves which shoaled the mixed layer. Another wind burst of comparable intensity occurred at the beginning of May 2000 while the thermocline was shallow, causing SST cooling at the equator (Fig. 13&14). However, the wind strengthening was less sudden than during the mid-May 2005 event and the resulting cooling took place over a less broad region (not shown). In addition, the surface pressure drop in the ITCZ region was not as pronounced as during mid-May 2005 event.

Ocean Sci. Discuss., https://doi.org/10.5194/os-2017-74
Manuscript under review for journal Ocean Sci.
Discussion started: 4 October 2017

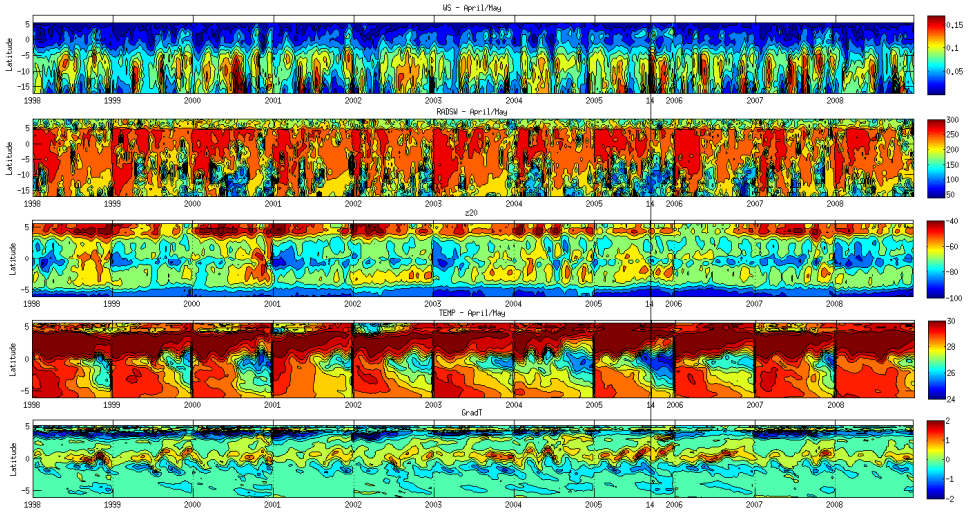

604

605 **Figure 13:** Time-latitude diagrams for April-May along the 1998-2008 period, of 2-days average, from top to
606 bottom, i) wind stress magnitude ($N.m^{-2}$) from CFSR fields; ii) short-wave radiation surface flux ($W.m^{-2}$) from
607 CFSR fields; iii) 20°C isotherm depth (m) computed from the forced model SST; iv) SST (°C) and v)
608 meridional SST gradient (every 0.5° of latitude), from the forced model; averaged over 10° W-6° W. The
609 vertical black line indicates the date of 14 May, 2005.

610

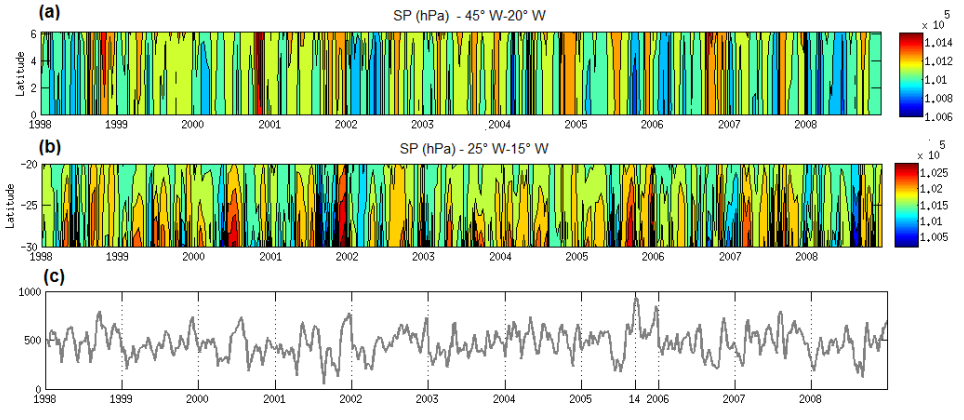

611

612 **Figure 14:** Time-latitude diagram, for April-May over the 1998-2008 period, of the surface pressure (hPa) from
613 ERA-20C reanalysis; (a) from 0° N to 6° N averaged between 45° W and 20° W ; and (b) from 30° S and 20° S
614 averaged between 25° W and 15° W; (c) differences between (a) and (b);.

615

Ocean Sci. Discuss., https://doi.org/10.5194/os-2017-74
Manuscript under review for journal Ocean Sci.
Discussion started: 4 October 2017

6. Summary and discussion

In this study, the impact of intraseasonal winds on SST in the far eastern Tropical Atlantic during boreal spring 2005 and 2006 has been investigated observations and numerical simulation. We first focus our study in Cape-Lopez region (CLR), east of 5°E and between the equator and 7° S, where the seasonal and interannual SST variability is poorly documented. There, the boreal spring (AMJ) season corresponds to a transitional period between high SST in boreal winter and weak SST in boreal summer, under the influence of local winds. Intensified cool SSTs are observed in the coastal upwelling area located around 6° S in the Congo mouth region, associated with mean alongshore wind conditions. Spring season is in fact characterized by maximum winds amplitude, influence of which is made more effective by shallow thermocline depth, itself strongly influenced by remote forcing. The seasonal cycle in the CLR is modulated by strong year-to-year variations, as observed in spring 2005 when cold SST anomaly are associated with shallower-than-average thermocline depth and positive wind speed anomaly.

The intraseasonal wind bursts which occurred in spring 2005 and 2006 generated cooling events especially around 3°-4° S but for some strongest events when the cooling reached more northern equatorial region, especially during the mid-May and end-May 2005 events. The intensity of the cold events resulted from both basin preconditioning by remotely forced shoaling of the thermocline (via Kelvin wave), local mixing (induced by current vertical shear) and upwelling processes in response to strong southerly local winds. For some particular event, as the 26-28 May 2005, the net heat flux also tended to cool the surface water, due to enhanced cloud cover which decreased the incoming solar radiations. In CLR, stronger wind intensification and favorably preconditioned oceanic subsurface conditions in 2005 made the coupling between surface and subsurface ocean processes more efficient than in 2006, resulting in stronger cooling.

The preconditioning of subsurface conditions in the area via Kelvin wave at the dates of the wind bursts depended on the atmospheric conditions in the western part of the basin a few weeks earlier. Previous studies (e.g. Picaut, 1983; Philander, 1990) suggest that the source of the equatorial Kelvin wave is mainly related to a sudden change of the zonal wind in the west. Analysis of atmospheric and oceanic conditions at intraseasonal to daily scale in winter 2005 and 2006 showed that for both years, Kelvin upwelling wave was initiated in the west while easterly winds were strengthened from either side of the equator just after the ITCZ to be at its southernmost location. This latter was observed one month earlier in 2006 (late February – early March) than in 2005 (late March-early April), and was associated with a negative wind stress curl anomaly. In winter 2005, the ITCZ was found south of the equator after a very sudden southward shift and was followed by strong easterlies during ~20 days, while in winter 2006, the ITCZ was found closer to the equator less sharply and during a longer period, followed by weaker easterlies when compared to 2005. These results obtained for 2005 and 2006 years do not imply that same atmospheric conditions would be observed for winter upwelling Kelvin wave of other years. Especially, the year 2005 was very particular and also exhibited anomalously cold SSTs in the south Atlantic and anomalously warm SSTs in the north Atlantic initiated in fall 2004, signature of a meridional mode (Virmani and Weisberg, 2006; Foltz and Mc. Phaden, 2006; Hormann and Brandt, 2009).

652 Upon impingement with the eastern boundary, the incoming equatorial Kelvin wave excites westward-
653 propagating Rossby waves and poleward propagating coastal Kelvin waves. In 2005, the Kelvin wave reached
654 the coast around mid-May while southerly winds strengthened, allowing the reflected wave to be reinforced by
655 the local wind. This resulted in westward propagation of positive (negative) z20 (SSH) anomalies which,
656 combined with enhanced westward surface currents, provided favorable conditions to westward extension of
657 cold upwelled water from the eastern coast to near 20°W through advection and vertical mixing.
658 In the second part of the study, we specially focused on the mid-May 2005 event (13 May to 16 May) that was
659 characterized by strong southerly wind strengthening in the eastern Tropical Atlantic Ocean. It was found to be
660 responsible for the sudden and intense SST cooling in the Gulf of Guinea and the CLR, and involved in the early
661 onset of the ACT development in 2005 and therefore in early onset of the WAM. The analysis of atmospheric
662 and oceanic conditions in the Gulf of Guinea associated to this event allowed to show that the mid-May event,
663 controlled by the St. Helena Anticyclone, can be identified as a "decisive event" which triggered the abrupt
664 transition between two wind patterns in the northern Gulf of Guinea. Unusual strong southerly winds induced
665 anomalously strong equatorial cooling which in turns slowed down the overlying wind feedback mechanism and
666 generated stronger than normal southerlies north of the equator through the SST front around 1°N. This
667 triggered the deep atmospheric convection in the Gulf of Guinea at a self-sustaining level and the beginning of
668 coastal precipitation. The time of occurrence of this phenomenon, 15 days earlier than the averaged date (31
669 May from Leduc-Leballeur et al., 2013), suggests than the mid-May 2005 event was associated with anomalous
670 strong moisture flux. The description of atmospheric conditions over the 1998-2008 period has shown that the
671 2005 event was characterized by the strongest surface pressure gradient between the St. Helena high pressures
672 and the low pressures under the ITCZ, inducing anomalous strong Hadley cell activity. No similar atmospheric
673 pattern was observed during the whole 1998-2008 period. Another wind burst of comparable wind intensity
674 occurred at the beginning of May 2000. This event also induced a cooling at the equator but the surface pressure
675 decrease in ITCZ region was not as pronounced than during mid-May 2005 event and the SST gradient around
676 1° N was weaker. In addition to coastal precipitation in the Gulf of Guinea and due to the early cooling in the
677 ACT region, unusually rainfall conditions also occurred between the northeast coast of Brazil and 15° W within
678 the SITCZ, which generally forms in early boreal summer.

679 Finally, this study highlights the impact of a strong southerly wind burst in the eastern tropical Atlantic during
680 boreal spring season, which is a transitional period during which an anomalous strong energy input may tip the
681 energy balance from an equilibrium state toward another one and thus impact the WAM system. The analysis of
682 atmospheric and oceanic conditions during the mid-May 2005 wind event allows to highlight the different
683 processes through which the wind power provided by the wind burst is brought to the ocean: i) direct effect of
684 the wind on the SST in the eastern tropical Atlantic, ii) energy transport via atmospheric gravity waves from
685 South Atlantic, and iii) energy supply to Rossby wave. In addition to unusual atmospheric conditions in mid-
686 May 2005, the ocean response intensity to this event was also enhanced by the subsurface conditions, made
687 favorable by previous wind bursts, either local (e.g. in 6-8 May) or occurring a few weeks before in the West.

It is crucial to better describe the atmospheric and oceanic processes in play during such extreme event, notably in order to reduce the well known warm bias in the southeastern tropics in coupled models in both atmospheric and oceanic components (Zeng et al., 1996; Davey et al., 2002; Deser et al., 2006; Chang et al., 2007; Richter and Xie, 2008). This warm bias is well evidenced in our numerical simulation (Fig. 1&2) and our results clearly show that the cooling events were underestimated in the CLR, implying the need to investigate more in depth the oceanic and atmospheric processes in play in this particular region. As the intraseasonal wind bursts are related to the fluctuations of St. Helena Anticyclone, their impact on SST variability in the eastern tropical Atlantic and regional climate suggests the need of better understand the St. Helena Anticyclone variability.

It is also important to note that the mid-May 2005 event occurred during an unusually active year. The year 2005 exhibited a pronounced meridional mode pattern with strong SST gradient between the two hemispheres. Several authors (Foltz et al., 2006 ; Virmani and Weisberg, 2006 ; Marengo et al., 2008a, 2008b ; Zeng et al., 2008) studied this particular year, marked by anomalously warm SST in the tropical North Atlantic during March-July, the warmest from at least 150 years. This anomalous warming was associated with the most active and destructive hurricane season on record (Foltz et al., 2006; Virmani and Weisberg, 2006) and an extreme and rare drought in the Amazon Basin (Marengo et al., 2008a, 2008b; Zeng et al. 2008; Erfanian et al., 2017). From these authors, primary causes of the anomalous warming in 2005 were a weakening of the northeasterly trade winds and associated decrease in wind-induced latent heat loss as well as changes in shortwave radiation and horizontal oceanic heat advection. This 2005 temperature record is made even more remarkable given that, unlike the 1998's one, it occurred in the absence of any strong El Niño anomaly (Shein, 2006). Some studies (Goldenberg et al., 2001) attribute these SST increases to the Atlantic Multidecadal Oscillation (AMO), while others suggest that climate change may instead be playing the dominant role (Emanuel, 2005; Webster et al., 2005; Mann and Emanuel, 2006; Trenberth and Shea, 2006). Comparable anomalously warm tropical Atlantic SSTs have been observed in 2010 also associated with extreme drought in the Amazon. However, from time series of monthly anomalies constructed for the two basins (North and South Atlantic) by using OISST monthly mean data, Erfanian et al. (2017) show that the warmer-than-usual SSTs in the North Atlantic in 2010 was not associated with colder-than-usual SST in South Atlantic contrarily to 2005 (their Fig. S4e).

While the warming in North Tropical Atlantic during 2005 has been investigated by several authors, the cooling in South Atlantic has received less attention. This study highlights the need to further document and monitor the South Atlantic region and the St. Helena Anticyclone, through additional high resolution analysis and observations.

Acknowledgments:

The research leading to these results received funding from the EU FP7/2007-2013 under grant agreement no. 603521, PREFACE and from the EU Horizon 2020 under grand agreement no. 2014-633211, AtlantOS. These

projects are gratefully acknowledged. We do thank Gildas Cambon for his help and participation on the implementation of ROMS simulations, and Frédéric Marin for his helpful comments.

References:

Adamec, D., O'Brien, J. J.: The seasonal upwelling in the Gulf of Guinea due to remote forcing, J. Phys. Oceanogr., 8, 1050-1060, 1978.

Battisti, DS.: Dynamics and thermodynamics of a warming event in a coupled tropical atmosphere ocean model, J. Atmos. Sci. 45:2889 – 2919, 1988.

Busalacchi, A., Picaut, J.: Seasonal variability from a model of the tropical Atlantic Ocean, J. Phys Oceanogr., 13, 1564-1588, 1983.

Bourlès, B., Brandt, P., Caniaux, G., Dengler, M., Gouriou, Y., Key, E., Lumpkin, R., Marin, F., Molinari, R.L., Schmid, C. : African Monsoon Multidisciplinary Analysis (AMMA): Special measurements in the Tropical Atlantic, CLIVAR Exchange Letters, 41 (12 2), International CLIVAR Project Office, National Oceanography Centre, Southampton, United Kingdom, 7–9, 2007.

Brandt, P., Funk, A., Hormann, V., Dengler, M., Greatbatch, R.J., Toole, J.M.: Interannual atmospheric variability forced by the deep equatorial Atlantic Ocean, Nature, 473, 497–500, doi:10.1038/nature10013, 2011.

Caniaux, G., Giordani, H., Redelsperger, J.-L., Guichard, F., Key, E., Wade, M.: Coupling between the Atlantic cold tongue and the West African monsoon in boreal spring and summer, J. Geophys. Res., 116, C04003, doi:10.1029/2010JC006570, 2011.

Carton, J. A., Chepurin, G., Cao, X., Giese, B.S.: A simple ocean data assimilation analysis of the global upper ocean 1950 –1995, part 1: Methodology, J. Phys. Oceanogr., 30, 294–309, doi:10.1175/ 1520-0485(2000)030<0294:ASODAA>2.0.CO;2, 2000a.

Carton, J. A., Chepurin, G., Cao, X.: A simple ocean data assimilation analysis of the global upper ocean 1950–1995, part 2: Results, J. Phys. Oceanogr., 30,311–326, doi:10.1175/1520-0485(2000) 030<0311:ASODAA>2.0.CO;2, 2000b.

760 Carton, J. A., and Giese, B.S.: A reanalysis of ocean climate using simple ocean data assimilation (SODA),
761 Mon. Weather Rev., 136 ,2999–3017, doi:10.1175/2007MWR1978.1, 2008.
762
763 Colin, C.: Sur la variabilité dans le Golfe de Guinée: Nouvelles considérations sur les mécanismes d'upwelling,
764 Ph.D. thesis, Mus. Natl. d'Hist. Nat., Paris, 1989.
765
766 Chang, C.-Y., Carton, J.A., Grodsky, S.A., Nigam, S.: Seasonal climate of the tropical Atlantic sector in the
767 NCAR Community Climate System Model 3: Error structure and probable causes of errors, J. Climate,
768 20, 1053–1070, 2007.
769
770 Chelton, D. B., deSzoeke, R.A., Schlax, M. G. , Naggar, K. E., Siwertz, N.: Geographical variability of the first-
771 baroclinic Rossby radius of deformation, J. Phys. Oceanogr., 28, 433–460, 1998.
772
773 Dai, A., and Trenberth, K.E.: Estimates of freshwater discharge from continents: Latitudinal and seasonal
774 variations, J. Hydrometeorol., 3, 660–687, 2002.
775
776 Davey, M., Huddleston, M., Sperber, K.R., et al.: STOIC: A study of coupled model climatology and variability
777 in tropical ocean regions, Clim. Dynam., 18, 403-420, 2002.
778
779 Debreu, L., Marchesiello, P., Penven, P., Cambon, G.: Two-way nesting in split-explicit ocean models:
780 algorithms, implementation and validation, Ocean Modelling, 49-50, 1-21, 2012.
781
782 De Coëtlogon, G., Janicot, S., Lazar, A.: Intraseasonal variability of the ocean-atmosphere coupling in the Gulf
783 of Guinea during boreal spring and summer, Q. J. R. Meteorol. Soc., 136, 426–441, doi:10.1002/qj.554,
784 2010.
785
786 Denamiel, C., Budgell, W.P., Toumi, R.: The Congo River plume: Impact of the forcing on the far-field and
787 near-field dynamics, J. Geophys. Res. Oceans, 118, 964–989, doi:10.1002/jgrc.20062, 2013.
788
789 Deser, C., Capotondi, A., Saravanan, R., Phillips, A.: Tropical Pacific and Atlantic climate variability in
790 CCSM3, J. Climate, 19, 2451–2481, 2006.
791
792 Djakouré, S., Penven, P., Bourlès, B., Veitch, J., Koné, V.: Coastally trapped eddies in the north of the Gulf of
793 Guinea, J. Geophys. Res. Oceans, 119, 6805–6819, doi:10.1002/2014JC010243, 2014.
794
795 Emanuel, K.: Increasing destructiveness of tropical cyclones over the past 30 years, Nature, 436, 686-688, 2005.
796

797 Erfanian, A., Wang, G., Fomenko, L.: Unprecedented drought over tropical South America in 2016:
798 significantly under-predicted by tropical SST, Scientific reports, 7:5811, doi: 10.1038/s41598-
799 017_05373-2, 2017.
800
801 Foltz, G. R., Grodsky, S. A., Carton, J. A., McPhaden, M. J.: Seasonal mixed layer heat budget of the tropical
802 Atlantic Ocean, J. Geophys. Res., 108, 3146, doi:10.1029/2002JC001584, 2003.
803
804 Foltz, G.R. and McPhaden, M.J.: Unusually warm sea surface temperatures in the tropical North Atlantic during
805 2005, Geophys. Res. Lett., 33: doi: 10.1029/2006GL027394. issn: 0094-8276, 2006.
806
807 Fritts, D. C.: Wave saturation in the middle atmosphere: A review of theory and observations, Rev. Geophys.,
808 22, 275–308, 1984.
809
810 Gentemann, C.L., Wentz, F.J., Brewer, M., et al.: Passive Microwave Remote Sensing of the Ocean: an
811 Overview, Oceanography from Space, Revisited, edited by V. Barale, J. Gower, and L. Alberotanza,
812 13–33. Heidelberg: Springer, 2010.
813
814 Giese, B.J, Harrison, D.E.: Aspects of the Kelvin wave response to episodic wind forcing, J. Geophys. Res., 95:
815 7289 – 7312, 1990.
816
817 Giordani, H., Caniaux, G., Voldoire, A.: Intraseasonal mixed-layer heat budget in the equatorial Atlantic during
818 the cold tongue development in 2006, J. Geophys. Res.: Oceans, 118(2):650-671. doi:
819 10.1029/2012JC008280, 2013.
820
821 Goldenberg, S.B., Landsea, C.W., Mestas-Nuñez, A.M., Gray, W.M.: The Recent Increase in Atlantic Hurricane
822 Activity: Causes and Implications, Sciences, Vol. 293, Issue 5529, pp. 474-479, doi:
823 10.1126/science.1060040, 2001.
824
825 Grodsky, S. A., Carton, J. A.: The Intertropical Convergence Zone in the South Atlantic and the Equatorial Cold
826 Tongue, J. Climate, 16, 723–733, 2003.
827
828 Haidvogel, D.B., Beckmann, A.: Numerical Ocean Circulation Modeling, Imperial College Press, London; 320
829 pp., 1999.
830
831 Herbert, G., Bourlès, B., Penven, P., Grelet, J.: New insights on the upper layer circulation north of the Gulf of
832 Guinea, J. Geophys. Res.: Oceans, 121, doi:10.1002/2016JC011959, 2016.
833

834 Hormann, V., Brandt, P.: Upper equatorial Atlantic variability during 2002 and 2005 associated with equatorial
835 Kelvin waves, J. Geophys. Res., 114: C03007, doi:10.1029/2008JC005101, 2009.
836
837 Illig, S., Dewitte, B., Ayoub, N., du Penhoat, Y., Reverdin, G., Mey, P.D., Bonjean, F., Lagerloef, G.S.E.:
838 Interannual long equatorial waves in the tropical Atlantic from a high-resolution ocean general
839 circulation model experiment in 1981-2000, J. Geophys. Res.: Oceans, 109:C02022. doi: 10.1029/
840 2003JC001771, 2004.
841
842 Jouanno, J., Marin, F., duPenhoat, Y., Sheinbaum, J., Molines, J.M.: Seasonal heat balance in the upper 100m of
843 the Equatorial Atlantic Ocean, J. Geophys. Res.: Oceans, 116:C09003. doi: 10.1029/2010JC006912,
844 2011.
845
846 Jouanno, J., Marin, F., duPenhoat, Y., Molines, J.M.: Intraseasonal Modulation of the Surface Cooling in the
847 Gulf of Guinea, J. Phys. Oceanogr., 43(2):382-401. doi: 10.1175/JPO-D-12-053.1, 2013.
848
849 Krishnamurti, T. N., Pasch, R.J., Ardanuy, P.: Prediction of African waves and specification of squall lines,
850 Tellus, 32, 215-231, 1980.
851
852 Leduc-Leballeur, M., Eymard, L., de Coëtlogon, G.: Observation of the marine atmospheric boundary layer in
853 the Gulf of Guinea during the 2006 boreal spring, Q. J. R. Meteorol. Soc., 137: 992 – 1003, 2011.
854 Leduc-Leballeur, M., de Coëtlogon, G., Eymard, L.: Air – sea interaction in the Gulf of Guinea at intraseasonal
855 time-scales: Wind bursts and coastal precipitation in boreal spring, Q. J. R. Meteorol. Soc., 139, 387–
856 400, doi:10.1002/qj.1981, 2013.
857
858 Lübbecke, J.F., Burls, N.J., Reason, C.J.C., McPhaden, M.J.: Variability in the South Atlantic Anticyclone and
859 the Atlantic Nino Mode, J. Climate, 27, doi: 10.1175/JCLI-D-14-00202.1, 2014.
860
861 Mann, M. E., and Emanuel, K.A.: Atlantic hurricane trends linked to climate change, Eos, Trans. Amer.
862 Geophys. Union, 87, 233–244, 2006.
863
864 Marengo, J. A., Nobre, C.A., Tomasella,J., Oyama, M.D., De Oliveira, G.S., De Oliveira, R., Camargo, H.,
865 Alves, L.M., Brown, I.F. : The drought of Amazonia in 2005, J. Climate, 21, 495-516, 2008a.
866
867 Marengo, J.A., Nobre, C.A., Tomasella, J., Cardoso, M.F., Oyama, M.D..: Hydro-climatic and ecological
868 behaviour of the drought of amazonia in 2005, Philosophical transactions of the Royal society of
869 London, Biological sciences, v.21, p.1-6, 2008b.
870

871 Marin, F., Caniaux, G., Bourlès, B., Giordani, H., Gouriou, Y., Key, E.: Why were sea surface temperatures so
872 different in the Eastern Equatorial Atlantic in June 2005 and 2006, J. Phys. Oceanogr., 39, 1416–1431,
873 doi:10.1175/2008JPO4030.1, 2009.
874
875 Materia, S., Gualdi, S., Navarra, A., Terray, L.: The effect of Congo River freshwater discharge on Eastern
876 Equatorial Atlantic climate variability, Clim. Dynam., 39(9-10), 2109–2125, doi:10.1007/s00382-012-
877 1514-x, 2012.
878
879 McCreary, J.: Eastern tropical ocean response to changing wind systems with application to El Nino, J. Phys.
880 Oceanogr., 6, 632-645, 1976.
881
882 McCreary, J., Picaut, J., Moore, D.: Effects of the remote annual forcing in the eastern tropical Atlantic Ocean,
883 J. Mar. Res., 42, 45 81, 1984.
884
885 Merle, J. : Conditions hydrologiques saisonnières de la marge continentale du Gabon et du Congo (de 10°N a
886 60°S) Etude descriptive, Dot. Sci. O.R.S.T.O.M. Pointe-Noire, 27 : l-20, 1972.
887
888 Merle, J., Fieux, M., Hisard, P.: Annual signal and interannual anomalies of sea surface temperature in the
889 eastern equatorial Atlantic Ocean, Deep Sea Res., 26,77–101, 1980.
890
891 Mitchell, T. P., Wallace, J.M.: The annual cycle in equatorial convection and sea surface temperature, J.
892 Climate, 5, 1140–1156, 1992.
893
894 Moore, D.W.: Planetary-gravity waves in an equatorial ocean, PhD Thesis, Harvard University, 201 pp., 1968.
895
896 Moore, D.W., and Philander, S.G.H.: Modeling of the tropical ocean circulation, The Sea, Vol. 6, Wiley
897 Interscience, New York, N.Y., pp. 316-361, 1977.
898
899 Moore, D. W., Hisard, P., McCreary, J. P., Merle, J., O'Brien, J. J., Picaut, J., Verstraete, J. M., Wunsch, C.:
900 Equatorial adjustment in the eastern Atlantic, Geophys. Res. Lett., 5, 637-640, 1978.
901
902 Nguyen, H., Thorncroft, C. D., Zhang, C.: Guinean coastal rainfall of the West African Monsoon, Q.J.R.
903 Meteorol. Soc., 137: 1828–1840. doi:10.1002/qj.867, 2011.
904 Nicholson, S.E., Dezfuli, A.K.: The relationship of rainfall variability in western equatorial Africa to the tropical
905 oceans and atmospheric circulation. Part I: The boreal spring, J. Climate, 26(1), 45–65, 2013.
906 Nobre, P., Shukla, J.: Variations of sea surface temperature, wind stress, and rainfall over the tropical Atlantic
907 and South America, J. Climate, 9 : 2464 – 2479, 1996.

Okumura, Y., and Xie, S.P.: Interaction of the Atlantic equatorial cold tongue and the African monsoon, J. Climate, 17, 3589–3602, 2004.

Okumura, Y., Xie, S.P.: Some overlooked features of tropical Atlantic climate leading to a new Niño-like phenomenon, J. Climate, 19(22), 5859–5874, doi:10.1175/JCLI3928.1, 2006.

Penven, P., Marchesiello, P., Debreu, L., Lefevre, J.: Software tools for pre- and post-processing of oceanic regional simulations, Environ. Modell. Software, 23, 2008 660–662, 2008.

Peter, A.-C., Le Hénaff, M., du Penhoat, Y., Menkès, C., Marin, F., Vialard, J., Caniaux, G., Lazar, A.: A model study of the seasonal mixed layer heat budget in the equatorial Atlantic, J. Geophys. Res., 111, C06014, doi: 10.1029/2005JC003157, 2006.

Philander, S., and Pacanowski, R.: A model of the seasonal cycle in the Tropical Atlantic Ocean, J. Geophys. Res., 91, 14, 192–14, 206, 1986.

Philander, S.G.: El Nino, La Nina and the Southern Oscillation, Academic Press, 293 pp., 1990.

Picaut, J.: Propagation of the seasonal upwelling in the eastern equatorial Atlantic, J. Phys. Oceanogr., 13, 18–37, doi: 10.1175/1520-0485, 1983.

Picaut, J.: On the dynamics of the thermal variations in the Gulf of Guinea, Oceanogr. Trop., 19 (2) : 127-53, 1984.

Piton, B. : Les courants sur le plateau continental devant Pointe-Noire (Congo), Documents scientifiques, ORSTOM, Brest, n°47, 37 p., 1988.

Polo, I., Lazar, A., Rodriguez-Fonseca, B., Arnault, S.: Oceanic Kelvin waves and tropical Atlantic intraseasonal variability: 1. Kelvin wave characterization, J. Geophys. Res., 113, C07009, doi: 10.1029/2007JC004495, 2008.

Redelsperger, J. L., et al. : AMMA: Une étude multidisciplinaire de la mousson Ouest-Africaine, Meteorologie, 54,22–32, doi:10.4267/2042/20098, 2006.

Richter, I. and Xie, S.-P.: On the origin of equatorial Atlantic biases in coupled general circulation models, Clim. Dynam., 1:587–598, doi : 10.1007/s00382-008-0364-z, 2008.

Rouault, M., Servain, J., Reason, C. J. R. , Bourlès, B., Rouault, M. J. , Fauchereau, N.: Extension of PIRATA in the tropical south-east Atlantic: An initial one-year experiment, Afr. J. Mar. Sci.,31(1),63–71, doi:10.2989/AJMS.2009.31.1.5.776, 2009.

Saha, S., Moorthi, S., Pan, H.-L., Wu, W., Wang, J., Nadiga, S., Tripp, P., Kistler, R., Woollen, J., Behringer, D., Liu, H., Stokes, D., Grumbine, R., Gayno, G., Wang, J., Hou, Y.T., Chuang, H.-Y., Juang, H.-M. H., Sela, J., Iredell, M., Treadon, R., Kleist, D., Van Delst, P., Keyser, D., Derber, J., Ek, M., Meng, J., Wei, H., Yang, R., Lord, S., Van Den Dool, H., Kumar, A., Wang, W., Long, C., Chelliah, M., Xue, Y., Huang, B., Schemm, J.-K., Ebisuzaki, W., Lin, R., Xie, P., Chen, M., Zhou, S., Higgins, W., Zou, C.-Z. Z., Liu, Q., Chen, Y., Han, Y., Cucurull, L., Reynolds, R.W., Rutledge, G., Goldberg, M. : The NCEP climate forecast system reanalysis, Amer. Meteor. Soc., 91, 1015-1057, 2010.

Schouten, M. W., Matano, R. P., Strub, T. P.: A description of the seasonal cycle of the equatorial Atlantic from altimeter data, Deep Sea Res., Part I, 52, 477–493, doi:10.1016/j.dsr.2004.10.007, 2005.

Servain, J., Picaut, J., Merle, J.: Evidence of remote forcing in the equatorial Atlantic Ocean, J. Phys. Oceanogr., 12, 457–463, 1982.

Shein, K. A.: State of the climate in 2005, Bull. Am. Meteorol. Soc., 87, s1–s102, doi: 10.1175/BAMS-87-6-shein, 2006.

Shchepetkin, A., McWilliams, J.C.: The Regional Oceanic Modeling System (ROMS): A split-explicit, free-surface, topography-following-coordinate ocean model, Ocean Modell. 9, 347–404, 2005.

Thorncroft, C. D., Nguyen, H., Zhang, C., Peyrillé, P.: Annual cycle of the West African monsoon: regional circulations and associated water vapour transport, Q. J. R. Meteorol. Soc., 137, 129-147, doi:10.1002/qj.728, 2011.

Trenberth, K.E., Shea, D.J.: Atlantic hurricanes and natural variability in 2005, Geophys. Res. Lett., vol. 33, L12704, doi: 10.1029/2006GL026894, 2006.

Virmani, J. I., and Weisberg, R.H.: The 2005 hurricane season: An echo of the past or a harbinger of the future?, Geophys. Res. Lett., 33, L05707, doi: 10.1029/2005GL025517, 2006.

Wade, M., Caniaux, G., du Penhoat, Y.: Variability of the mixed layer heat budget in the eastern equatorial Atlantic during 2005–2007 as inferred using Argo floats, J. Geophys. Res., 116, C08006, doi: 10.1029/2010JC006683, 2011.

Yu, L., Jin, X., Weller, R.A.: Role of net surface heat flux in seasonal variations of sea surface temperature in the tropical Atlantic ocean, J. Climate, 19, 6153–6169, 2006.

Waliser, D. E., and Gautier, C.: A satellite-derived climatology of the ITCZ, J. Climate, 6, 2162–2174, 1993.

Wauthy, B. : Introduction à la climatologie du Golfe de Guinée, Oceanogr. Trop., 18, 103–138, 1983.

Webster, P.J., Holland, G. J., Curry, A., Chang, H.R.: Changes in tropical cyclone number, duration, and intensity, in warming environment, Science, 309, 1844-1846, 2005.

Wentz, F.J., and. Meissner, T.: Algorithm Theoretical Basis Document (ATBD), version 2, AMSR-E Ocean Algorithm, Remote Sensing Systems Tech. Rep., RSS 121599A-1, 55 pp., 2000.

White, R.H. and Toumi, R.: River Flow and Ocean Temperatures: The Congo River, J. Geophys. Res. -Oceans, 119, 25016–2517, doi:10.1002/2014JC009836, 2014.

Zebiak, S.: Air-sea interaction in the equatorial Atlantic region, J. Climate, 6(8), 1567–1586, doi:10.1175/1520-0442(1993)006<1567:AIITEA>2.0.CO;2, 1993.

Zeng, N., Dickinson, R.E., Zeng, X.: Climatic impact of Amazon deforestation-A mechanistic model study, J. Climate, 9, 859–883, 1996.

Zeng, N., Dickinson, R.E., Zeng, X.: Causes and impacts of the 2005 Amazon drought, Env. Res. Lett., 3, doi: 10.1088/1748-9326/3/1/014002, 2008.